NANO · MICRO small
www.small-journal.com

Photonics and Optoelectronics of 2D Metal-Halide Perovskites

Xiang Qi, Yupeng Zhang, Qingdong Ou, Son Tung Ha, Cheng-Wei Qiu, Han Zhang, Yi-Bing Cheng, Qihua Xiong,* and Qiaoliang Bao**

In the growing list of 2D semiconductors as potential successors to silicon in future devices, metal-halide perovskites have recently joined the family. Unlike other conversional 2D covalent semiconductors such as graphene, transition metal dichalcogenides, black phosphorus, etc., 2D perovskites are ionic materials, affording many distinct properties of their own, including high photoluminescence quantum efficiency, balanced large exciton binding energy and oscillator strength, and long carrier diffusion length. These unique properties make 2D perovskites potential candidates for optoelectronic and photonic devices such as solar cells, light-emitting diodes, photodetectors, nanolasers, waveguides, modulators, and so on, which represent a relatively new but exciting and rapidly expanding area of research. In this Review, the recent advances in emerging 2D metal-halide perovskites and their applications in the fields of optoelectronics and photonics are summarized and insights into the future direction of these fields are offered.

1. Introduction

Metal-halide perovskites, the subordinate of perovskites adopting the formula ABX_3, have emerged as energy-efficient, low-cost materials.[1–4] To start with pure perovskite $CsSnI_3$ and its analogues, the diversity of structural and chemical variability of organic–inorganic hybrid perovskites promotes paramount opportunities in photonics and optoelectronics.[5–9] In recent years, metal-halide perovskites, in which A denotes an organic or inorganic monovalent cation, and B and X are replaced by a bivalent cation (Pb^{2+}, Sn^{2+}, or Ge^{2+}) and a halogen (Cl^-, Br^-, and I^-), respectively, have exhibited great promises in photonics and optoelectronics applications since the first report by Miyasaka and co-workers in the application of dye-sensitized solar cells.[10] Owing to their high optical absorption coefficient, low nonradiative recombination rate, long carrier diffusion lengths, high photoluminescence quantum yield, and outstanding tunable optical properties, metal-halide perovskites possess intriguing potential in optoelectronic applications such as photodetectors, solar cells and light-emitting diodes (LEDs), and others photonic devices.[11–13] In particular, perovskite film-based planar photodetectors exhibited high gain, fast response time, and flexibility, indicating their considerable promise in next-generation high-performance photodetectors.[14–16] Besides that, the perovskite film-based LEDs were reported to achieve an efficiency of 42.0 candela per ampere, which is already comparable to that of state-of-the-art organic LEDs.[17,18] The fascinating developments in graphene research[19–21] have rapidly stimulated many other 2D materials, including black phosphorus,[22,23] silicene,[24,25] hexagonal boron nitride (h-BN),[26,27] and transition metal dichalcogenides (TMDs).[28,29] 2D semiconductor materials have received significant attention due to the strong quantum confinement and the tunable large bandgaps in these materials, which are desired for many photonic and optoelectronic applications.[30–34] Similarly, perovskites with 2D

Dr. X. Qi, Dr. Y. Zhang, Prof. C.-W. Qiu, Prof. H. Zhang, Prof. Q. Bao
College of Electronic Science and Technology
College of Optoelectronics Engineering
SZU-NUS Collaborative Innovation Centre for Optoelectronic Science & Technology, and Key Laboratory of Optoelectronic Devices and Systems of Ministry of Education and Guangdong Province
Shenzhen University
Shenzhen 518000, China
E-mail: ypzhang@szu.edu.cn

Dr. X. Qi, Dr. Y. Zhang, Dr. Q. Ou, Prof. Y.-B. Cheng, Prof. Q. Bao
Department of Materials Science and Engineering
Monash University
Wellington Road, Clayton, Victoria 3800, Australia
E-mail: qiaoliang.bao@monash.edu

The ORCID identification number(s) for the author(s) of this article can be found under https://doi.org/10.1002/smll.201800682.

DOI: 10.1002/smll.201800682

Dr. X. Qi
Hunan Key Laboratory of Micro-Nano Energy Materials and Devices and School of Physics and Optoelectronics
Xiangtan University
Hunan 411105, P. R. China

Dr. S. T. Ha, Prof. Q. Xiong
Division of Physics and Applied Physics
School of Physical and Mathematical Sciences
Nanyang Technological University
Singapore 637371, Singapore
E-mail: qihua@ntu.edu.sg

Prof. C.-W. Qiu
Department of Electrical and Computer Engineering
National University of Singapore
4 Engineering Drive 3, Singapore 117583, Singapore

configuration have evoked enormous attentions in the fundamental understanding on its physical properties and optoelectronic applications.[35] The early works on using the excellent optical gain properties of 2D perovskites have opened a wide range of opportunities in photonic applications.

Derived from the parent bulk metal-halide perovskite, the thickness and electronic structure can be controlled by adjusting the stoichiometry of each perovskite lattice unit or site.[36–40] The study which involves synthesizing perovskites with 2D configurations is imperative for truly understanding their photophysics in integrated optoelectronic devices.[41,42] Distinct from covalent contenders, 2D perovskites, including layered and nonlayered forms, are ionic materials, which exhibit prominent fluorescence emission decay rates compared to many conventional semiconductors.[43] It has been proven that the large surface area of in-plane perovskite structures enables a stronger interaction with other materials for efficient charge or energy transfer, which benefits multiple photonic and optoelectronic functions of light generation, emission, transmission, and detection.[41,43–45] Over the past few years, significant progress has been made in the field of 2D perovskites and in their related optical and optoelectronic devices.[46–48] Following the demonstrations of the state-of-the-art pure perovskites with both high efficiency as well as stability,[36,39] further breakthroughs are expected by following optimization and a better fundamental understanding upon the internal electron dynamics and corresponding interfacial engineering.

This Review aims to provide an up-to-date summary of recent advances in emerging 2D metal-halide perovskites and their applications in the fields of optoelectronics and photonics and to offer our insights into the future direction of these fields. We hope this Review can give a novel perspective to trigger new possibilities in the conceptual development of novel 2D metal-halide perovskite materials, architectures, and devices, which would provide a rational contribution to fundamental studies of perovskite photonics and optoelectronics and inspire the production of new 2D metal-halide perovskites with superior photonic and optoelectronic performances.

2. Emergence of 2D Metal-Halide Perovskites

Perovskites are a large family of compounds that are named after Lev A. Perovski, the Russian Count, by the German mineralogist Gustav Rose who had first discovered the mineral $CaTiO_3$.[49] Since the previous exploration in 1880,[50] the surge of hybrid perovskites shares the common chemical formula ABX_3 beginning with the well-known characterization of $MAPbX_3$ in 1978, in which MA denote methylammonium and X is a halide anion.[51,52] Metal-halide perovskites, as revealed by the name, are constructed by an inorganic halide (I^-, Cl^-, Br^-) that occupies the anion X site. An alternative organic or inorganic monovalent A^+ cation would form inorganic (A = inorganic) and hybrid (A = organic) metal-halide perovskites, respectively. More importantly, the crystal stacking of perovskite can be easily turned from 3D bonded structure to 2D layered structure with weak van der Waals (vDW) forces, through varying the A^+ cations.[53,54] When the A lattice site is occupied by a small monovalent

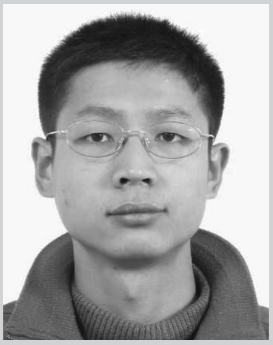

Xiang Qi received his B.S. degree in Physics (2004) and Ph.D. in Materials Physics and Chemistry (2009) from the School of Physics and Technology, Wuhan University (China). He joined the School of Physical and Optoelectronics, Xiangtan University (China) as a lecturer in 2009, and was appointed as an associate professor since 2011. He was a visiting scholar at Department of Materials Science and Engineering, Monash University from 2016 to 2017. His research currently focuses on the controlled synthesis and optoelectronic devices of 2D materials.

Qihua Xiong received his B.S. degree in Physics from Wuhan University (1997), and his M.S. degree from Shanghai Institute of Applied Physics, Chinese Academy of Sciences (2000). He obtained his Ph.D. under the supervision of Peter C. Eklund from the Pennsylvania State University (2006). After three years postdoctoral experience in Charles M. Lieber's group at Harvard University, he joined Nanyang Technological University as an assistant professor (2009). He was tenured and promoted to Nanyang Associate Professor in 2014 and was promoted to full professor in 2016. His research focuses on light–matter interactions of emergent quantum matter by optical spectroscopy approaches.

Qiaoliang Bao received his B.A. (2000) and M.E. (2003) degrees in Materials Science and Engineering from Wuhan University of Technology (China). He obtained his Ph.D. (2007) in Materials Physics and Chemistry from Wuhan University (China). He worked as postdoctoral fellow at Nanyang Technological University and National University of Singapore from 2007 to 2012. He is currently an associate professor at Department of Materials Science and Engineering, Monash University. His research interests include synthesis and optical characterization of 2D materials as well as their incorporation into photonic and optoelectronic devices.

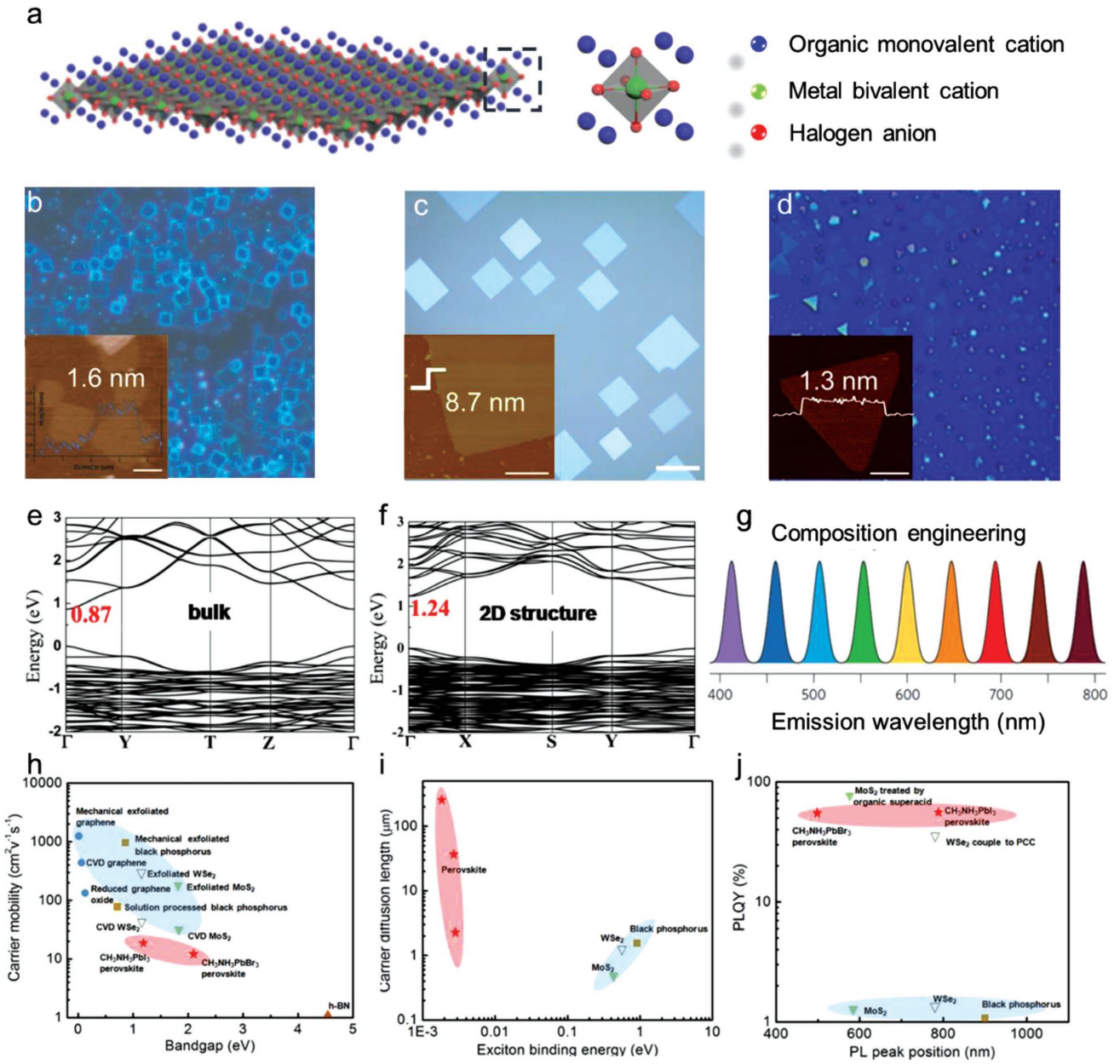

Figure 1. a) Structure models of 2D perovskite nanosheets. b) Optical and AFM image of 2D $(C_4H_9NH_3)_2PbBr_4$ nanosheets produced via solution processing. Reproduced with permission.[41] Copyright 2015, American Association for the Advancement of Science. c) Optical and AFM image of 2D $CH_3NH_3PbCl_3$ nanosheets produced via a one-step chemical vapor deposition (CVD) method with dual precursor sources. Reproduced with permission.[56] Copyright 2015, American Chemical Society. d) Optical and AFM image of 2D $CH_3NH_3PbI_3$ nanosheets produced via a combination of solution processing and a subsequent vapor-phase conversion. Reproduced with permission.[41] Copyright 2016, American Chemical Society (scale bars of optical images in (b)–(d): 10 μm; scale bars of optical images in (b)–(d): 1 μm). Band structures for the e) bulk and f) 2D $MAPbI_3$ calculated by the vdW-DF functional and spin–orbit coupling approach. Reproduced with permission.[81] Copyright 2015, American Chemical Society. g) Emission wavelength, h) carrier mobility,[88–90] i) carrier diffusion length,[91–93] and j) photoluminescence quantum yield of 2D perovskite and other 2D covalent semiconductors.[99–102]

cation, such as Cs, $CH_3NH_3^+$ (MA^+), $HC(NH_2)_2^+$ (FA^+), 3D symmetry is achieved. Whereas in case of a larger cation, such as $CH_3CH_2NH_3^+$, $(C_4H_9NH_3)_2^{2+}$, 2D structures can be obtained. To produce perovskites with different structures, a series of synthesis methods have been reported toward 2D structures with specific unit cells, even with single-unit-cell thickness (**Figure 1**a). Dou et al.[41] fabricated high-quality organic–inorganic perovskite $(C_4H_9NH_3)_2PbBr_4$ nanosheets from solution using a ternary cosolvent. In general, the solvent medium in the solution process is the key factor that affects the crystallinity, morphology, and texture of the precipitated crystals. By controlling the ratio of dimethylformamide/chlorobenzene/acetonitrile cosolvent, the dissolution and crystallization of perovskite can be balanced. As a result, the atomically

thin 2D perovskites (Figure 1b) with square shapes can grow on different substrates such as Si/SiO_2, Si, quartz, mica, etc. This study opens up opportunities for fundamental research on the synthesis and characterization of atomically thin 2D metal-halide perovskites and introduces a new family of 2D solution-processed semiconductors for nanoscale optoelectronic devices. But such approach lacks processibility on size, shape, and composition engineering, and the products are rather polydisperse. In the case of perovskite with 3D bonded structure, instead of atomically thin layers, thin nanocrystals with random shapes would be formed by solution process due to the structural property. Therefore, methods of obtaining non-vDW perovskites with several unit cells thickness (less than 10 nm), which have higher photovoltaic performance and a broader range of applications, are also of strategic interest. Recently, Ha et al. first developed chemical vapor deposition (CVD) synthesis of perovskite nanoplatelets on mica substrate based upon a vDW epitaxy mechanism.[55] This method was further employed by Wang and co-workers[56] to push the sample thickness (below 10 nm) on mica substrates (Figure 1c). The weak material–substrate interaction and low cohesive energy of the perovskite lead to the growth of large-scale ultrathin 2D crystals. Another effective approach to prepare atomically thin non-vDW 2D perovskites has been demonstrated by Liu et al.,[45] in which 2D PbI_2 nanoplatelets were first prepared in oversaturated solution followed by a vapor-phase conversion of PbI_2 to $MAPbI_3$ through the intercalation of MAI. Due to the 2D layered structure with weak vDW forces in PbI_2, the thickness of the as-prepared 2D perovskite could be modulated by controlling the thickness of the initial 2D PbI_2 nanoplatelets (Figure 1d). The vapor phase one-step and two-step synthetic approaches are both powerful, and they together provide extra flexibility in making new 2D perovskites and heterostructures. However, producing single crystal/large area, high quality 2D perovskites with well-defined few or single-unit-cell thickness and desired chemical compositions is still challenged. It is thus highly demanded to develop scalable synthesis methods for the production of 2D perovskites with high quality and processibility for their applications.

The breakthrough in the synthesis makes 2D perovskite a highly promising material for various practical applications. However, the unstable nature and abundant dangling bonds on the surface will accelerate the degradation of 2D perovskite in ambient environments, which hinder the long-term use. Preparation of 2D perovskites with enhanced stability has thus been a critical challenge that must be tackled to drive 2D perovskite-based devices toward next level applications. It is noteworthy that Tsai et al. reported a phase pure Ruddlesden–Popper layered perovskites with a stability more than 2250 h in solar cell devices.[36] The long and bulkier hydrophobic organic group on the surface of perovskite can prevent the direct exposure to moisture, significantly improving the stability. Besides that, considering the instability of organic cations, all-inorganic 2D perovskite, such as $CsPbX_3$, has drawn much attention due to superior environmental and thermal stability in air. Zeng and co-workers[57] reported that large-scale 2D $CsPbX_3$ perovskite nanoplatelets with a thickness as low as 1.7 nm can be produced and they demonstrated conspicuous optoelectronic performance as well as preferable stability. Recently, Fan et al. revealed the atomistic mechanism for the degradation in perovskite microplates[58] by in situ transmission electron microscope (TEM) observations combined with the density functional theory (DFT) simulations. It was confirmed that the surface reaction initiates layer-by-layer degradation pathway during the perovskite decomposition. In this regard, the surface treatment in terms of dangling bonds passivation can effectively address the stability issue as well. Based on the experience in bulk perovskite films, incorporation of organic molecules, such as alkyl halide or oleic acid,[59] to enhance perovskite surface passivation is an important direction for future progress. Furthermore, the encapsulation of the 2D perovskites with 2D materials (i.e., graphene, boron nitride, etc.) which are impermeable will also help to suppress the surface degradation.

3. Optical and Electronic Properties

Metal-halide perovskites have attracted intensive attention primarily because of their excellent optical and electronic properties. The variety in chemical composition of the perovskite family can realize a facile way to fine-tune the physical properties including bandgap, electrical conductivity, excitonic behavior, etc. Aside from the identical thickness-dependent band structure as that in traditional 2D semiconductors, the bandgap of metal-halide perovskites can be engineered by adjusting the chemical composition, allowing vast absorption across visible and near-infrared wavelengths. In particular, the nature of as-produced metal-halide perovskites is highly sensitive toward preparation scheme and precursor choice. The favorite optoelectronic properties can be achieved by lowering the concentration of defect sites in perovskite crystals which can greatly suppress the nonradiative recombination of excited carriers and result in increased photoluminescence quantum yield. In this regard, low-dimensional perovskites have shown competitive photoluminescence (PL) and electroluminescence (EL) efficiency compared with bulk perovskite films, primarily benefiting from lower density of defects and higher exciton binding energies. Alternatively, the optoelectronic properties can also be rationally adjusted by controlling the morphology of metal-halide perovskites, particularly when applied as light absorber for solar cells. In solar cell devices, the exciton recombination rate associated with exciton diffusion length can significantly influence the power conversion efficiency.[60] Tan and co-workers suggested a highly efficient trimethylaluminum vapor-based cross-linking method to produce $CsPbX_3$ nanocrystals (NC). The cross-linked NC films were insoluble, which allowed the deposition of subsequent charge-injection layers without orthogonal solvents. Therefore, the high quality NC film coverage with the confinement of injected charges within the perovskite crystals facilitated electron–hole recombination, thus yielding remarkable external quantum efficiencies (EQEs) and light emission properties.[61] In addition, long Auger lifetime and low stimulated emission threshold have been observed in perovskite recently, which may promote the exploration of integrated optical applications.[48] In general, the high absorption coefficient, strong photoluminescence, and long carrier diffusion length in metal-halide perovskites make them favorable for numerous optoelectronic and photonic applications, including solar cells, LEDs, lasing applications, and photodetectors.[45,62–71]

3.1. Band Structure and Optical Transitions

The metal-halide perovskite crystal can be viewed as an anion corner-shared 3D network of $(BX_6)^{4-}$ octahedra, with B cations at their centers and A cations between them. Generally, the A cation is proposed to have no direct contribution toward the electronic properties of perovskites, and the band structures of perovskites are mainly correlated with the largest metal–halide–metal bond angle, which can be adjusted by the BX_6 octahedral tilting, based on theoretical investigations.[72] Figure 1e shows the band structures for the bulk $MAPbI_3$ calculated by the van der Waals density functional (vdW-DF) and spin–orbit coupling approach. The valence band maximum consists of antibonding states derived from hybridizations of the atomic 5p orbitals of iodine and 6s orbitals of lead, whereas the conduction band minimum is mainly formed of empty 6p orbitals of lead. The heavy nature of the lead and iodine ions leads to significant spin–orbit coupling and thus lower the bandgap. An important difference between the band structures of the bulk and 2D perovskites lies in the bandgap energy. It can be seen that the bandgap energy of 2D perovskites is 0.37 eV larger than that of the bulk (Figure 1f), which has also been experimentally verified.[41,45,73] For the perovskites either with 3D bonded structure or 2D layer structure, reducing the thickness to atomically thin leads to an increase in the bandgap due to the size-induced or quantum confinement.[41,74] The nature of increase in the bandgap for hybrid perovskite 2D sheets can be attributed into a strong in-plane crystal structure distortion in hybrid perovskites, which is relatively different from conventional semiconductors (i.e., CdS, MoS_2).

The electronic structure of 2D metal-halide perovskites can also be tuned by composition engineering, as that in the bulk counterparts.[75,76] Substitution of the halide anion with increasing atomic size (Cl–Br–I) will lead to a decrease in the bandgap.[75] Similarly, substitution of the organic cation will shift the absorption onset energy downward while increasing cation size.[54,77] However, opposite effects are found when the metal cation was replaced by larger cation. The absorption onset shifts downward from 1.6 to 1.2 eV when the larger lead cation is replaced with the smaller tin cation.[78,79] Consequently, the absorption and emission of 2D perovskites can be well tuned from 400 to 800 nm, which covers the entire visible wavelength range (Figure 1g).

3.2. Optoelectronic Properties

The carrier mobility of 2D perovskite is rather modest (about 6–60 $cm^2\ V^{-1}\ s^{-1}$), at least one order of magnitude lower than that of conversional 2D covalent semiconductors (Figure 1h).[80–82] As a result, the carrier lifetime of perovskite can be as long as several hundred nanoseconds (even microseconds), and the carrier diffusion length is up to micrometer scale for both electrons and holes (Figure 1i).[83–85] Such promising optoelectronic performances are initiated from slow trap and/or surface-state emission and associated with structural crystallization. These unexpected phenomena are mainly associated with the spontaneous generation of free electrons and holes following photoabsorption, as well as the multiple absorption–diffusion–emission (photo recycling) effect,[86–88] which creates high excitation densities and behaves in an unusual way from those in conversional 2D covalent semiconductors. In addition, the high absorption coefficients, together with direct bandgap regardless the thickness of 2D perovskites, result in a relatively high photoluminescence quantum yield (PLQY). This is also distinct from conversional 2D covalent semiconductors (Figure 1j).[89–92] The PLQY can be substantially enhanced through spatial confinement of charges, the use of a scaffold, the passivation of perovskite surface, etc., which are crucial for the development of high performance lasers and LEDs.

3.3. Ion Migration

Ion migration in perovskites has been suggested to be an important factor for many unusual behaviors in perovskite-based optoelectronics, such as current–voltage hysteresis, low-frequency giant dielectric response, and the switchable photovoltaic effect. Especially for the 2D perovskites, ions migration is confined into the 2D plane, which should amplify the influence. Previous studies revealed that ion migration, especially the migration of organic cations in low-dimensional perovskites,[93] will induce a reversible structural swell–shrink. This will recoverably affect the reflective index,[93] absorption/color,[94] quantum efficiency, light-harvesting, and photoelectric properties,[95] making 2D perovskite a promising candidate for constructing tunable photonic or optoelectronic devices, such as ultrafast, entirely solid-state displays with nanometer-scale pixels, semi-transparent smart glasses, smart contact lenses, and artificial retina devices.[96]

4. Heterostructures

The large and well-defined surfaces of 2D materials endow strong surface interaction with adjacent materials, which is better suited for assembly into heterosturctures. Recent investigations on heterostructures composed of 2D perovskites and conventional 2D material crystals have attracted considerable interest.[97,98] Because of the large number of 2D crystals (including graphene, TMDs, metal nanosheets, etc.), it is possible to create a substantial variety of heterostructures based on 2D perovskites. Mechanical assembly technique may be attractive due to the formation of clean interface contact over large areas, whereas the low productivity greatly hindered its practical applications.[21,99] Similar to the synthesis of individual 2D perovskites, the vapor-phase deposition method has been used for the controlled fabrication of perovskite platelets on other 2D materials. Niu et al. used semimetallic graphene (**Figure 2**a–c), semiconducting MoS_2 (Figure 2d–f), and insulating h-BN (Figure 2g–i) as substrates for growing $CH_3NH_3PbI_3$ nanoplatelets to form various 2D perovskite-based heterostructures.[100] Such vertical heterostructures have been grown in this scalable fashion and designed to depict superior performance from the synergistic effect between high charge mobility of conventional 2D materials and improved interface engineering effectiveness. In particular, $MAPbI_3$ film was

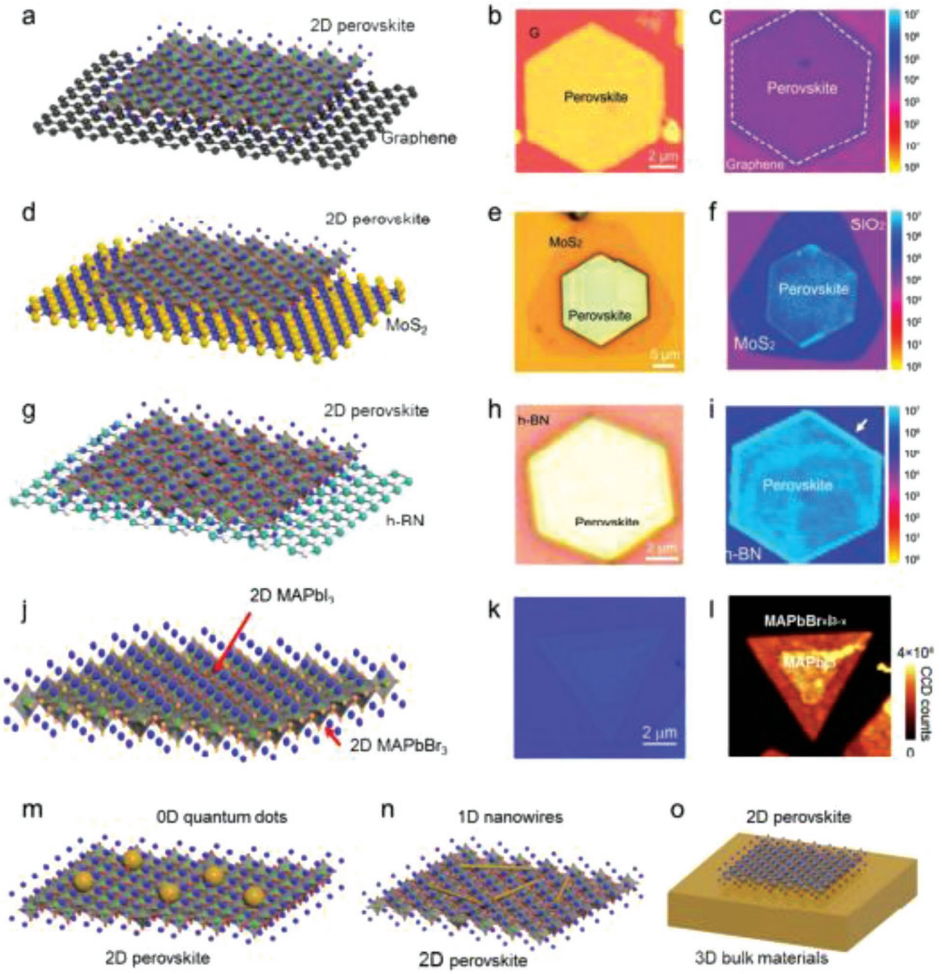

Figure 2. a) Structure models, b) optical image, and c) PL mapping of the perovskite/graphene vertical heterostructures. d) Structure models, e) optical image, and f) PL mapping of the perovskite/ MoS_2 vertical heterostructure. g) Structure models, h) optical image, and i) Raman intensity mapping of the perovskite/h-BN vertical heterostructure. Reproduced with permission.[100] Copyright 2015, John Wiley and Sons. j) Structure models, k) optical image, and l) PL mapping of the $CH_3NH_3PbI_3/CH_3NH_3PbBr_xI_{3-x}$ in-plane heterostructure. Reproduced with permission.[45] Copyright 2016, American Chemical Society. Structure models of mixed-dimensional heterostructures between a 2D perovskite and m) 0D semiconductors, n) 1D materials, or o) 3D semiconductors.

deposited on the surface of single-layer graphene, and the high photoresponsivity (180 A W^{-1}) and EQE (5×10^4%) may be resulted from the enhanced electron transfer from graphene to $MAPbI_3$ and reduce electron–hole recombination under photoexcitation.[101,102]

Unlike conventional 2D materials-based heterostructure, metal-halide perovskites can form heterostructures with broadly changed chemical composition but maintain a similar crystal structure. By halide-exchange reaction, a series of mixed halide perovskite ($MAPbBr_{3-x}Cl_x$ or $MAPbBr_{3-x}I_x$) heterostructures with tuneable bandgap over a wide range (1.6–3.0 eV) can be obtained, which makes them promising for optoelectronic applications operating in a wide wavelength range.[103] One interesting example is the in-plane heterostructure consisting of $CH_3NH_3PbI_3$ and $CH_3NH_3PbBr_xI_{3-x}$, as shown in Figure 2j–l,[45] in which different regions give the light emission at different wavelengths. Dou et al. fabricated $CsPbX_3$ nanowire heterostructure via anion exchange, revealing competitive benefit such as tuneable optical characteristics and multicolor display.[104] Inspired by the unique optoelectronic properties of different perovskite structures, material with identical dimensional geometries can be used to create mixed-dimensional heterostructure geometries[105,106] (2D–0D, 2D–1D, and 2D–3D, as shown in Figure 2m–o), which is proposed to unlock a new paradigm for nanoscale material integration and the development of extraordinary applications.

5. Optoelectronic Applications

5.1. Photodetectors

As mentioned above, the high solar-to-energy conversion efficiency and other outstanding features of perovskites promise superior performance for photodetection. A wide range of perovskite-based materials from thin films to single crystals have

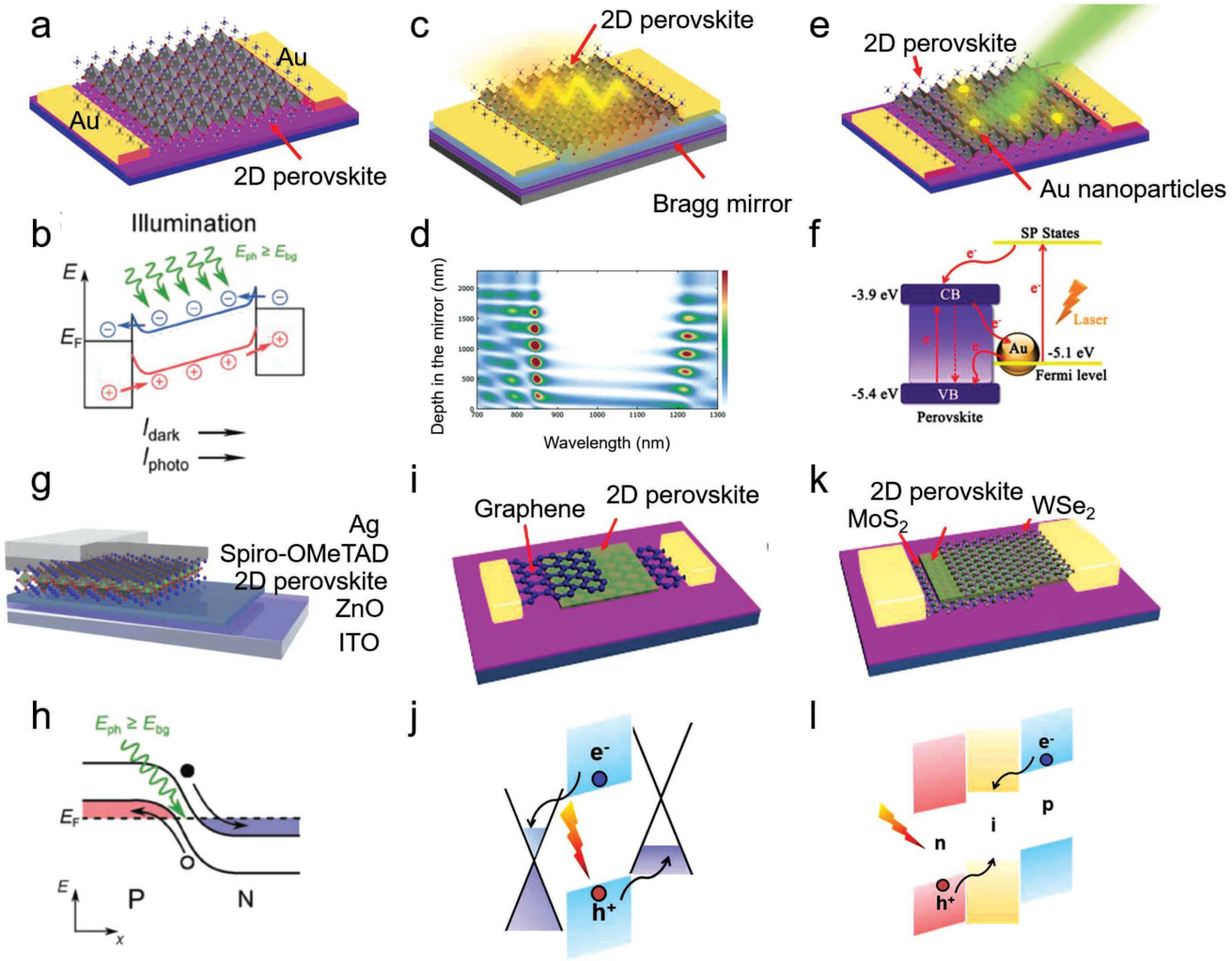

Figure 3. Design of novel 2D perovskite based photodetectors. a) Schematic illustration and b) band diagram of a typical 2D perovskite-based photodetector with a mesa configuration. c) Schematic model and d) band diagram of a 2D perovskite-based photodetector with asymmetric metal contacts. e) Schematic illustration and f) band diagram of a typical 2D perovskite-based photodetector with a vertical configuration. g) Schematic model and j) enhanced mechanism of a 2D perovskite microcavity photodetector. h) Schematic drawings and k) enhanced mechanism of the hybrid 2D perovskite-quantum dots photodetector. i) Schematic illustration and l) band diagram the 2D perovskite based plasmon enhanced photodetector. m) Schematic illustration and p) band diagram of the graphene/perovskite/graphene vertical type photodetectors. n) Schematic illustration and q) band diagram of the MoS_2/perovskite/WSe_2 vertical type photodetectors. o) Schematic illustration and r) band diagram of p–n junction diode photodetector based on dual gate.

been gradually explored for fabricating the detection of visible light as well as X/gamma rays.[107–109] However, bulk films consisting of sub-microscale or nanoscale tiny perovskite particles would introduce a large number of grain boundaries and result in the formation of significant electron and photon scattering centres in photodetectors, which leads to problems such as low efficiency and responsivity. The photoresponsivity and detectivity of photodetector can be determined by equations, $R = I_{ph}/PS$ and $D = S^{1/2} \times R/(2eI_d)^{1/2}$, respectively, where R is photoresponsivity, I_{ph} is photocurrent density, P is power density, S is surface area, I_d is dark current density.[110] Attempts to address this issue are of utmost importance for perovskite-based photodetectors with improved figure of merits. Using high quality 2D perovskites as photoactive media in photodetection devices is an efficient approach to address those problems.

Generally, the operation of 2D perovskite photodetectors has two mechanisms: photoconductive and photovoltaic effect. In case of photoconductive regime where perovskite is a photoconductor, light absorption produces additional free carriers, which reduces the electrical resistance of the perovskite. **Figure 3**a shows a representative photoconductive device based on 2D perovskite and Figure 3b schematically illustrates operation mechanism. Since more than one electron can flow in consequence of a single absorbed photon, an EQE higher than 100% is possible, due to the mismatch between the charge recombination time and the charge transit time (photoconductive gain). The high EQE leads to high photocurrent, and consequently, high responsivity, making this type of photodetector remarkably promising for application in highly efficient detection and high-resolution imaging. For instance, the 2D perovskite

$MAPbI_3$ nanosheet device with symmetric gold electrodes showed a high photoresponsivity of 22 A W^{-1} under visible laser excitation, representing a better performance than that of photodetectors based on bulk perovskite films.[45] Application of graphene film as transparent electrodes further led to a high responsivity of ≈2100 A W^{-1} for the photodetector based on individual 2D $(C_4H_9NH_3)_2PbBr_4$ perovskite crystals.[111] Lateral photoconductive devices have additional advantages that are typically much more reproducible and easier for production. Photodetector array based on wafer-scale perovskite microplates has been demonstrated by selective growth of perovskites on prepatterned electrode arrays.[53] The lateral photoconductor devices also afford a high compatibility with flexible or wearable substrates, e.g., photodetector based on $CsPbBr_3$ nanosheets having >10 000 bendable cycles, while maintaining high photodetection performance.[112]

High gain is a specific feature of photodetectors operating on photoconductive effect (especially photogating effect). Electrical gating is a widely used method to realize high gain of a photoconductor. Engineering the gate dielectrics would also be an effective route to modulate the carrier concentration in the channel and the on/off ratio of the photodetector. Using thinner high-κ dielectrics and liquid/solid ionic dielectrics would also result in a higher gating efficiency.[113] Meanwhile, by manipulating the piezo-phototronic effect, piezoelectric dielectrics have been used to modulate the sensitivity of photodetectors.[114] In addition, to introduce photonic cavity (Figure 3c,d) and plasmonic resonance (Figure 3e,f) into the 2D perovskite photodetector offers alternatively effective approach to enhance the absorption as well as photocarrier generation. Although the high EQE and responsivity can be achieved in photoconductive mode, the large electrode spacing requires a relatively high working voltage to maintain high gain, which remarkably increases the dark current and sacrifices the performance in terms of detectivity. The high working voltage may also induce the ions migration in 2D perovskite, leading to unpredictable effects on its microstructure as well as device performance.

For the photovoltaic effect (photodiode), photogenerated electron–hole pairs are separated by an internal electric field that is usually accompanied in a p–n junction (Figure 3g,h). Generally, in photodiodes, an absorbed photon can generate at best one electron–hole pair with an EQE of no more than 100%. Therefore, the introduction of interface layers (electron-transport and hole-transport layers) cannot guarantee in the improvement of photoresponsivity, but can effectively reduce the dark current to obtain high detectivity. Alternatively, vertical photodiodes are generally built on p–n junctions or heterostructures with charge transport layers, as shown in Figure 3g,h. In such a photodiode, the built-in electric field within the perovskite channel (i.e., depletion region) is favorable to the generation, separation, transport, and collection of the photogenerated carriers. Perovskite photodetectors based on vertical bulk heterojunctions have shown unprecedented performance, for example, high photoresponsivity (242 A W^{-1}[115]), high detectivity (10^{14} Jones[116]), high EQE (≈90%[117]), and short response time (120 ns.[117]). The electrons and holes in the vertical-type devices have much shorter transport distances to the electrodes than those in the lateral devices, which results in quicker photoresponse.[118] In particular, 2D perovskites with ultrathin thickness and large in-plane surface areas afford short ion migration path and ultralarge depletion width, which are beneficial for making vertical-type photodiodes. However, the construction of vertical-type devices requires more patterning steps during fabrication compared to the lateral ones.

Combination of 2D perovskites with conventional 2D materials offers an effective route to engineer the surface and interface properties so as to enhance the extraction of photocarriers through the suppression of the photoexcited electron–hole recombination in the perovskite layer.[119,120] The sandwiching of 2D perovskites in between two graphene layers (Figure 3i,j) or other 2D materials layers (MoS_2, WSe_2, etc., Figure 3k,l) with gradient energy levels could create a built-in electric field or form a p–i–n structure. This will facilitate the separation of photoexcited electron–hole pairs across the heterostructures and realize highly efficient photocurrent generation. By applying different bias voltages at different parts of the perovskite sheet or film, excellent photoresponse properties, high sensitivity with a light on/off ratio, and outstanding flexibility can be expected. However, the sluggish response time and low linear dynamic range are the major issues preventing pervoskite-based photodetectors for practical applications. To address these problems, the engineering of the gate dielectric can be an effective route to modulate the carrier concentration in the channel and the on/off ratio of the transistor. In addition, interface engineering can be fascinated through the abovementioned methods. For example, the insertion of a BN layer between the coupled perovskite heterostructure can minimize the trapping state, while the redistribution of ions in the 2D heterosystems may have an overwhelming tuning effect on the photovoltaic effect and efficiency.[121]

5.2. Solar Cells

Recently, extensive reports have focused on metal-halide perovskite solar cells and have described the basic fundamentals of perovskite materials, device structures, and preparation technics to gain a better understanding of high performance perovskite solar cells.[11,40,122–124] Despite the certified efficiency of 22.1%,[125] perovskite cells are still prone to degradation in moisture, heat, oxygen, and ultraviolet light. To this end, new device or chemical engineering approaches are desired to improve the stability of 2D perovskites so as to suit for application demands. Owing to its unique atomic and chemical structures, 2D perovskite with smooth surface and large chemically active interface would exhibit a larger tunability in its optoelectronic properties, which can provide feasibility to construct solar cells with vertical configurations.

2D Ruddlesden–Popper phase layered perovskites with large alkyl ammonium cations have shown superior moisture stability over solely 3D methylammonium-based perovskites.[126,127] Aligning the crystalline planes along the out-of-plane orientation, which facilitates efficient carrier transport along the perovskite planes, results in high-efficiency solar cells with improved moisture and light stability, such as over 17.5% achieved by introducing 2D butylammonium perovskite grains.[128] Several mechanisms contribute to the improved stability including passivation of the

grain boundaries by long-chain layered perovskite phase, increased crystallinity, and reduced crystal defects. Besides stability aspects, 2D perovskites exhibit higher optical quality and quantum yield compared with bulk materials and larger carrier diffusion length compared with their quantum dots counterpart. More importantly, extremely efficient internal exciton dissociation have been unveiled to occur through edge states in 2D perovskites,[129] which provide a direct pathway for dissociating excitons into longer-lived free carriers that substantially improve the performance of optoelectronic devices.

To achieve efficiencies beyond the single-junction limit, the fabrication of tandem devices is a commonly used strategy. A tandem cell is a unique form of solar cell that consists of two or more sub-cells, where sub-cells stacked on top of one another absorb complementary portion of the sunlight spectrum. 2D perovskite could be a smart choice for the top cell when combined with either silicon or copper indium gallium selenide (CIGS) bottom solar cells, as the perovskite top cell possessing ultrathin smooth surface absorbs visible light but transmits infrared and near infrared light to the bottom cell,[130] as shown in **Figure 4**a,b. Meanwhile, the optical bandgap of 2D perovskite can be tuned via halide replacement, cation exchange, and lead substitution. Therefore, it is possible to realize tandem devices by using the same family of perovskite materials, for example, a $CH_3NH_3PbBr_3$–$CH_3NH_3PbI_3$ tandem structure,[131] as show in Figure 4c,d. Through bandgap engineering and matching, perovskite–perovskite tandem solar cells achieved an efficiency of 20.3% efficiency in mechanically stacked four tandem cells.[132] Insertion of monolayer/few-layer h-BN film as cationic diffusion barrier between $CH_3NH_3SnI_3$ and $CH_3NH_3PbI_{3-x}Br_x$ led to a graded bandgap solar cell with a high efficiency of 21.7%.[121] Further introduction of graphene as electrodes allows us to fabricate highly transparent and flexible tandem perovskite solar cells. The tandem device design sheds light on the purport of "all perovskite" tandem solar cells for the aim to reach the utmost efficiencies along with long term stability at the lowest costs.

5.3. LEDs

Halide perovskites exhibit superior light emission characteristics across visible and near-infrared wavelengths, including high photoluminescence quantum yield, broad spectra tunability, and high color purity, making them a competitive candidate for applications in LEDs. However, the efficiency of perovskite LEDs is inherently limited by the low exciton binding energy-induced facile dissociation of excitons in bulk perovskites.[14,18,133] To improve the electron-to-photon conversion efficiency, 2D perovskites with a large exciton binding energy stand out and offer an efficient alternative to enhancing radiative recombination. The first perovskite LED was demonstrated as early as 1994,[134] showing the potential of realizing high luminance intensity (10 000 cd m^{-2}) based on the layered $(C_6H_5C_2H_4NH_3)_2PbI_4$ perovskite. However, the low exciton binding energy in bulk perovskites would inherently hamper further improvements in the electron–photon conversion efficiency.[14,18,133] To develop high-efficiency LEDs, ultrathin active regions or low-dimensional perovskite emitters are needed to spatially confine carriers and thereby enhance radiative recombination. Figure 4e,f depicts the representative device structure of the 2D perovskite-based LED and the corresponding energy-level diagram, comprising a 2D perovskite emitting layer in a double-heterojunction structure with hole/electron transport

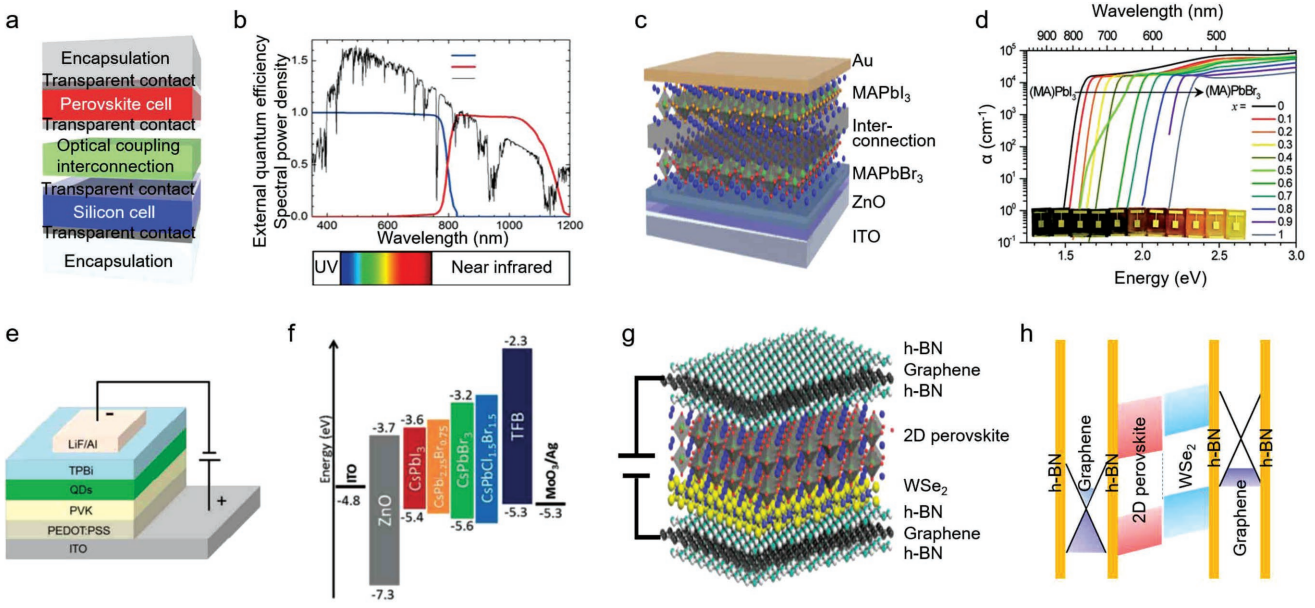

Figure 4. a,b) Schematic model of a representative 2D perovskite-based solar cell combined with either silicon or CIGS bottom solar cells. Reproduced with permission.[130] Copyright 2014, Institute of Electrical and Electronics Engineers. c,d) Schematic illustration of a 2D perovskite tandem solar cell, where each heterojunction absorbs different parts of the incoming sunlight. Reproduced with permission.[131] Copyright 2015, The Royal Society of Chemistry. e) Schematic model and f) corresponding energy-level diagram for a typical perovskite-based LED. Reproduced with permission.[14] Copyright 2015, John Wiley and Sons. g) Schematic drawing and h) corresponding band diagram of the perovskite LED based on 2D heterostructure.

layers. Tuning of the chemical composition and thickness of 2D perovskite emitters yields spectrally tuneable light-emitting properties while proper design of device architectures and interface engineering lead to enhanced electroluminescence efficiency. Most LEDs based on 2D perovskites used this sandwiched device structure (p–i–n stack) and achieved significant improvement in external quantum efficiency, such as 0.48% by mixing perovskite platelets in a polymer matrix,[135] 8.8% via perovskite energy funnels,[71] and 11.7% based on self-organized perovskite multiple quantum wells.[136]

From the perspective of 2D materials, inspired by the high EQE of 8.4% obtained in vertical heterostructures based on graphene/h-BN/TMD/h-BN/graphene quantum well,[137] we propose an atomically thin 2D perovskite quantum-well LED that can be built by carefully designing stacked 2D materials with customized band structures, as shown in Figure 4g,h. For 2D Ruddlesden–Popper-type perovskites, the optical properties can be tuned by adjusting the thickness of quantum well structure.[138] A typical 2D perovskite quantum-well LED consists of a heterostructured active layer sandwiched by insulating h-BN as tunnelling layers and metallic graphene as electrodes. This configuration has many merits such as balanced carrier injection, improved recombination of spatially confined excitons, enhanced photon extraction through transparent h-BN and graphene, and enhanced stability by self-encapsulation. Combining the tandem solar-cell configuration (Figure 4c) and quantum-well stack (Figure 4g), one can build 2D perovskite-based tandem LEDs that emit monochromatic light with doubled efficiency or emit white light by using perovskites with complementary emission, which are unexplored and urgently required both fundamentally and technologically for perovskite-based lighting and displays.

6. Photonics Applications

6.1. Nanolasers

Lasing occurs when a high gain material is placed in a suitable optical cavity. Since the discovery of amplified spontaneous emission in perovskites,[139] many studies have been conducted to explore their potential application in lasers. An early attempt involved placing the material on top of a distributed Bragg reflector, which amplified the emission to achieve lasing.[140] Another approach is to use the perovskite crystal as a naturally formed cavity. Zhang et al. first demonstrated that perovskite nanoplatelets can act as a whispering-gallery-mode cavity, and they achieved lasing in the infrared regime without using an artificial optical cavity (**Figure 5**a–c).[69] It can be clearly observed that the diffraction patterns inside the perovskite nanoplatelets with different shapes denote whispering-gallery-mode (Figure 5b). The patterns located inside the corresponding nanoplatelets appear in relatively smaller areas but are of similar shapes as the nanoplatelets, which indicate good optical confinement. The lasing spectra in Figure 5c further resolve different whispering-gallery modes. The log–log scale plot of the emission intensity and pumping power depict an *S*-like shape and the ultrafast decay of the photoluminescence lifetime (inset in Figure 5c), which further confirm the lasing in the perovskite nanoplatelets. This result is particularly of interest due to their potential applications in nanoscale optoelectronics.

Recently, the same group also realized high-quality whispering-gallery-mode lasing in 2D inorganic caesium lead halide perovskite nanoplatelets, which exhibit a low linewidth (≈0.14 nm), a low threshold (2.0 cm^{-2}), and a tunable lasing range from the ultraviolet to near infrared regimes.[141] By manipulating the halide content in the perovskite composition, it is possible to precisely control the emission wavelength and achieve lasing in all visible spectra (Figure 5d). Impressively, Zhu et al.[142] demonstrated lasing in $CH_3NH_3PbX_3$ with an exceptionally low threshold of only 220 nJ cm^{-2}, which corresponds to a carrier density as low as 1.5×10^{16} cm^{-3}. Another remarkable property of halide perovskite is the extremely low carrier trapping sites, and the estimated lasing quantum yield is close to 100%. In addition to the high optical gain, the high-quality crystalline structure of 2D perovskites is responsible for its high performance as a self-lasing material. With their exceptional coherent light emission and the ambipolar charge transport properties, perovskite materials may someday be applied in electrically driven lasing. Recent comprehensive review articles on perovskite-based lasing can be referred to ref. [143].

6.2. Grating

Grating is typical for photonic devices, in which the patterned periodic structure is required to modulate or control the light–matter interaction. Using focused-ion beam patterning, Alias et al.[144,145] demonstrated the fabrication of binary and circular sub-wavelength grating reflectors on the $MAPbBr_3$ perovskite crystal, and all the grating dimensions (the period, duty cycle, and grating thickness) were patterned with nanoscale precision (>63 nm), high contrast, and excellent uniformity. It was found that the perovskite-based grating reflector typically exhibits high reflectivity (>90%) and a broadband spectrum (400–1100 nm) for both transverse electric and transverse magnetic polarizations. 2D perovskites with planar structures could be an ideal platform to artificially fabricate ultrathin gratings and other planer photonic nanostructures or nanodevices with nanoscale precision.

6.3. Waveguides

A waveguide is a structure that guides waves, such as electromagnetic waves or sound, with minimal loss of energy by restricting expansion to one dimension or two. Generally, there are two types of optical interconnects, i.e., silica-based passive waveguide and luminescent material based active waveguide. In order to develop active waveguides with good performance, novel optical materials with high quantum yield of PL, large stimulated emission cross-section, and chemically tunable light emission are desired. In this regard, perovskites have been investigated as high performance active optical waveguides with a small propagation loss. The first active optical waveguide was demonstrated in 1D perovskite polycrystalline nanowires, in which the guiding of light with different colors was achieved

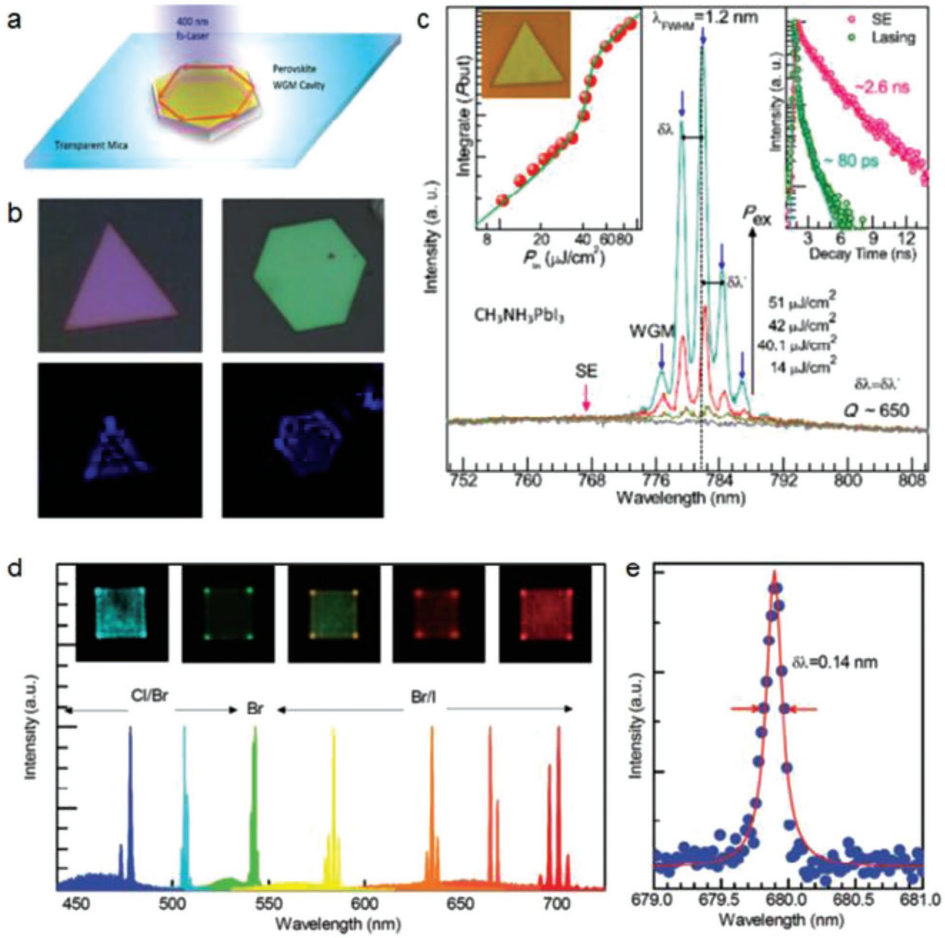

Figure 5. Optical lasing in lead halide perovskite nanoplatelets. a) Schematic of optical setup. A pulsed laser (400 nm, 150 fs, 1 kHz) globally excites the sample from the top globally. b) Far-field optical image of two typical nanoplatelets under the illumination of white light (upper panel) and an incident laser (bottom panel). c) The evolution from spontaneous emission to lasing in a triangular perovskite nanoplatelet. Reproduced with permission.[69] Copyright 2014, American Society of Chemistry. d) Lasing spectra and images of individual square perovskite nanoplatelets with different halide compositions. e) The full width at half maximum of the lasing mode is only 0.14 nm. Reproduced with permission.[141] Copyright 2016, John Wiley and Sons.

by fabricating high-quality perovskite with different halogen elements.[146] In addition, in a highly uniform monocrystalline perovskite nanowire, the optical field would be well-confined inside the cavity, creating a whispering gallery mode waveguide. It is noteworthy that the corresponding propagation loss is roughly 0.04 dB μm^{-1} for a propagation distance of 100 μm, which is much better than that of polycrystalline perovskite nanowires and other traditional semiconductor nanowires.[147]

As the 2D perovskite has a relatively large planar area and good pocessability, it provides the possibility for further processing into functional photonic devices and integrating with existing on-chip systems. In particular, Y-junction waveguides, microring modulators, and M–Z interferometers can be fabricated. By elemental doping or electrical gating, the electronic structure as well as reflective index of perovskite waveguide can be locally changed so that the light emission and propagation can be modulated. These emerging characteristics will stimulate the designing of a number of optical devices used for signal processing or optical sensing.

6.4. Lenses

Lenses are an indispensable component in almost all aspects of science and technology, including imaging, sensing, communications, and medical diagnosis and treatment. With the rapid development in nanooptics and on-chip photonic systems, the development of ultrathin flat lenses with a 3D sub-wavelength focusing capability, a large operational bandwidth, and practical focusing efficiency is highly desired. Based on the tunable refractive index of perovskites induced by ion migration, novel ultrathin lenses based on 2D perovskites are anticipated to effectively and simultaneously manipulate the phase and amplitude of an incident beam. Researchers have fabricated a $CH_3NH_3PbI_3$ nanosheet-based lens via a mask-free focused-ion beam method, and the preliminary results indicate that a tunable refractive index would be achieved under an applied electrical field.[144] However, similar with other 2D materials, the insufficient phase or amplitude modulation based on the intrinsic refractive index and low absorption of the materials

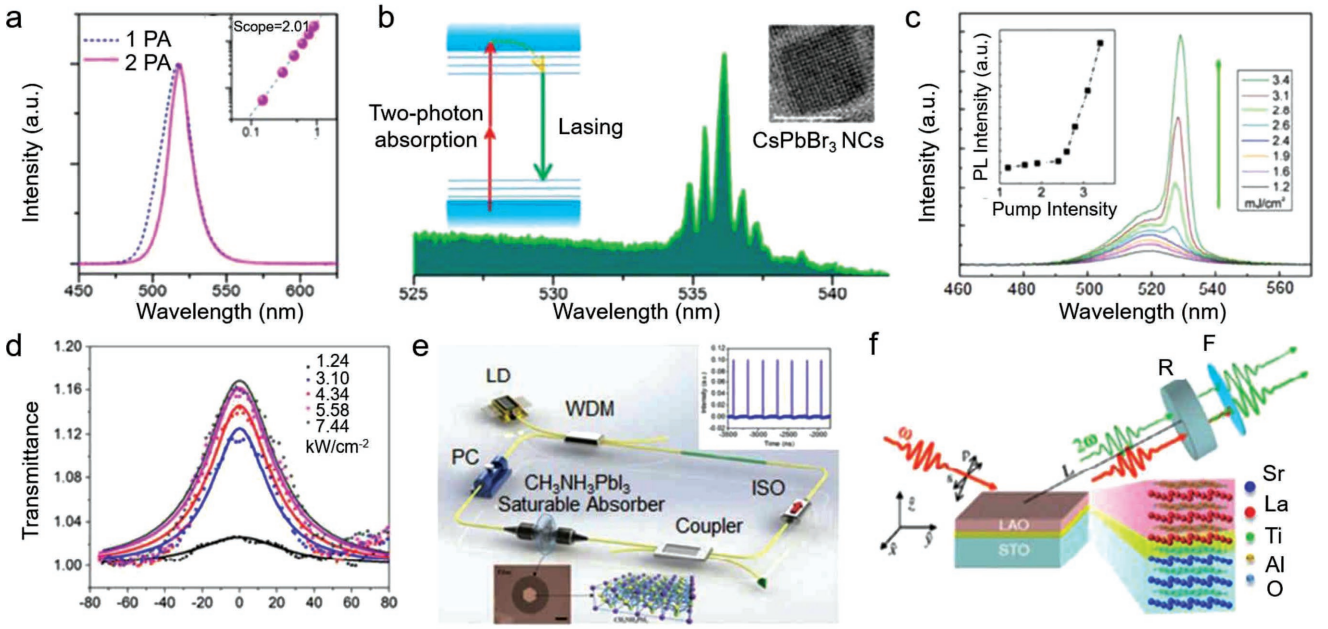

Figure 6. a) Normalized PL spectra recorded under one-photon and two-photon excitations recorded from a drop-cast film of $CsPbBr_3$ nanocrystals. The inset shows the quadratic dependence of PL emission on the fluence of two-photon excitation. b) Schematic view of the physic process of two-photon-pumped lasers. Reproduced with permission.[154] Copyright 2016, American Chemical Society. c) Three-photon pumped PL spectra from $CsPbBr_3$ nanocrystals under excitation wavelength of 1250 nm and varied pump intensities. Reproduced with permission.[155] Copyright 2015, American Chemical Society. d) Experimental results and theoretical fitting for the saturable absorption of 2D $CH_3NH_3PbI_3$ perovskite by an open-aperture Z-scan setup of a 800 nm laser under different pumping intensities. e) Schematic diagram of the ring cavity of the mode-locked fibre laser using a 2D perovskite as a saturable absorber (upper inset: output pulse trains of the mode-locked dissipative soliton. Bottom inset: optical image of the perovskite nanosheet on fiber. The scale bar is 25 μm). Reproduced with permission.[70] Copyright 2017, American Chemical Society. f) Schematic view of second harmonic generation experiment in $LaAlO_3/SrTiO_3$ (LAO/STO) thin film. Reproduced with permission.[158] Copyright 2015, American Physical Society.

results in poor performance when the thickness is reduced to sub-nanometer. Therefore, it is required to introduce sufficient phase or amplitude modulation to achieve high performance ultrathin flat lens. Introducing the innovative concepts, such as metasurface, metamaterial, or superoscillations, into the 2D materials based flat lens is thus expected. Apart from the aforementioned applications, the precision patterning of 2D perovskites via mask-free direct laser writing or focused-ion beam methods would also be used to enhance light trapping and absorption in perovskite solar cells and photodetectors to increase the power conversion efficiency.

6.5. Nonlinear Optics

Apart from the optoelectronic and photonic applications mentioned above, the nonlinear optical properties of 2D perovskites have not been entirely explored. Owing to the centosymmetry of the perovskite unit cell, the second-order susceptibility $\chi^{(2)}$ is generally absent at room temperature.[148,149] However, the third-order nonlinear processes, in principle, are allowed in all materials. It was recently estimated that the nonlinear refractive index in $CH_3NH_3PbI_3$ could be $\approx 36 \times 10^{-12}$ cm^2 W^{-1} for nonresonant femtosecond excitation,[150] and the third-order nonlinear susceptibility in $CH_3NH_3PbBr_3$ could be $1.6 \pm 1.0 \times 10^{-6}$ esu,[151] which have the same order of magnitude as observed for the semiconductors that are typically used in optical switches such as GaAs and Si.

There are previous encouraging reports about nonlinearities in various types of metal-halide perovskites.[149–153] Perovskite semiconductor NC films have demonstrated the potentials to tackle current challenges such as the two-photon-based pumped lasers and optical modulations. Whispering gallery mode lasing under two-photon pumping of perovskite $CsPbBr_3$ NCs films had been successfully realized by incorporating it in microcapillary resonators. A large cross-section of two-photon absorption at 800 nm ($\approx 2.7 \times 10^6$ GM) of $CsPbBr_3$ NCs films should account for the amplified spontaneous emission with a remarkable low threshold value ($\approx$0.8 mJ cm^{-2}) and modal gain coefficient (>500 cm^{-1}) in the frequency up-conversion (**Figure 6**a,b).[154] Furthermore, perovskite NC film shows low threshold frequency up-converted stimulated emission pumped by three-photon absorption, as shown in Figure 6c. The stability of stimulated emission and tunable wavelength by composition makes it to be a promising light source used in a wide frequency range.[155]

Compared to its bulk counterparts and thin NCs films, 2D metal-halide perovskites are more suitable for investigating intrinsic nonlinear optical properties for its relatively small photocarriers recombination and nonlinear scattering.[70] The nonlinear absorption coefficient of 2D perovskite nanosheet is two orders of magnitude larger than that of the bulk perovskite, and 2D perovskite is able to achieve mode locking at lower power threshold than bulk one, as shown in Figure 6d. Moreover, the modulation depth of 2D perovskites at 1028 nm is ≈31%, which is much higher than that of few-layers MoS_2

(10.47%).[156] and comparable to few-layers graphene.[157] By transferring suitable 2D perovskite nanosheets onto the end facet of an optical fibre ferrule to fabricate a saturable absorber, a ultrafast picosecond pulses can be generated,[70] as shown in Figure 6e. However, the nonlinear property such as second harmonic generation (SHG) has been rarely reported in emerging perovskite with form AMX_3. Nevertheless, SHG-based laser has been obtained from the interface of conventional perovskite films ($LaAlO_3/SrTiO_3$) (Figure 6f),[158] and in principle, it can be expected to yield SHG in these novel perovskite films for lasing by stacking different materials or crystalline mixing.[159]

By considering the saturable absorption effect based on the small nonlinear absorption coefficients of perovskites, the output power and repetition rate of $CH_3NH_3PbI_3$ and $CH_3NH_3PbI_{3-x}Cl_x$ thin film could increase as the pump power raised, resulting in a maximum output power of 29 mW in the range of 99–237 kHz and shortened temporal pulse width decrease of 305 ns, which is typical for passive Q-switching.[149]

To fully use the advantages provided by the nonlinear properties of perovskite, mature techniques for stable and environmentally friendly fabrication of perovskite are demanded. Moreover, long-term stability of metal-halide perovskite in moist environment is a paramount challenge to realize the commercialization of perovskite optical devices, while integrating graphene or other 2D transitional metal dichalcogenides on perovskite films may provide a viable solution to this problem and improve their properties.[160]

7. Summary and Perspectives

Metal-halide perovskites have attracted considerable attention over the past few years, but the investigation of the physical properties in their 2D forms is a relatively new and exciting area for potential optoelectronic and photonic applications. The superior optoelectronic properties and high power conversion efficiencies of metal-halide perovskites make them attractive, while the strong quantum confinement in 2D perovskites is promising for the field of optoelectronics and photonics. In this Review, the recent developments in 2D metal-halide perovskites, as well as their optoelectronic and photonic applications, have been broadly summarized. Despite the impressive improvements in 2D metal-halide perovskites over the past few years, their applications in optoelectronics and photonics are still hindered by a number of challenging issues. We hope that our discussion in this Review will aid the design of novel 2D perovskites and the development of related optoelectronic and photonic devices with desired performances.

7.1. Controllable Synthesis

Up to now, several synthetic methods have been explored for fabricating 2D perovskites, whereas these methods have struggled to satisfy the desired requirements for particular applications. Xiong and co-workers demonstrated a two-step vapor-phase deposition method to fabricate 2D $MAPbI_3$, in which 2D PbI_2 nanoplatelets were first deposited followed by a vapor-phase conversion of PbI2 to $MAPbI_3$ through the intercalation of MAI.[55] Unlike the 2D perovskite prepared via the one-step CVD growth, the thickness of the as-prepared 2D perovskite could be modulated by adjusting the thickness of the initial 2D PbI_2 nanoplatelets. Meanwhile, the photoluminescence of the mixed halide lead perovskite could also be tuned over a broad wavelength range from the visible to near infrared regimes by adjusting the conversion process conditions, such as the pressure and temperature. In this case, sustainable efforts should be made to achieve a scalable and controllable sample fabrication technique to produce large amounts of thickness-controlled and uniform 2D metal-halide perovskites, either in solution or on substrates.

7.2. Stability

In addition, stability of 2D perovskites remains a critical issue for particular applications. Recent advances have demonstrated that the stability of perovskites can be remarkably improved through chemical passivation and surface-ligand termination, but much more attention on this issue is required to improve the long-term stability of perovskite materials and the reproducibility of perovskite-based devices. In addition to the instability, the replacement of toxic Pb with environmentally friendly elements is also a major concern for the production of perovskite materials and devices that would be used in daily life. Nontoxic Sn and Bi have been shown to share comparatively similar properties to Pb, but they appear to be relatively unstable, which further hinders their ultimate optical and electronic properties.

7.3. Dynamics

In addition, 2D perovskites, unlike most 2D covalent semiconductors, are special ionic materials where ion-migration behavior is general and intrinsic to the perovskites.[93,94,161] Drawing upon the previous research on bulk perovskite materials, future research efforts are required to investigate the fundamental material properties of 2D perovskites and, in particular, the charge-carrier dynamics and ion-migration behaviors in this confined 2D system. Furthermore, the correlation between the structure and property still demands an in-depth exploration, which in turn would guide the rational design and precise manipulation of the optical and electronic properties.

7.4. Applications

Moreover, recent investigations mainly focused on the linear optical properties and related devices, and the excellent nonlinear optical properties of perovskites have clearly indicated a desired promise in broadband optical limiting and ultrafast photonic devices. Furthermore, techniques developed for graphene and other 2D materials can be implemented to generate unique properties of perovskites, and novel optoelectronic and photonic devices with various configurations would be designed. We believe that the deep investigation of 2D perovskite and their unique properties, which are distinct from other material systems, will open an avenue for their

unexpected and promising applications in practical optoelectronics and photonics.

Acknowledgements

The authors acknowledge the support from ARC (Grant Nos. FT150100450, IH150100006, and CE170100039), the National Key Research & Development Program (Grant No. 2016YFA0201902), and the National Natural Science Foundation of China (Grant Nos. 51290273, 1433107, and 51702219). Q.X. gratefully acknowledges the support from Singapore National Research Foundation via NRF Investigatorship Award (Grant No. NRF-NRFI2015-03) and Ministry of Education via AcRF Tier2 grant (Grant No. MOE2015-T2-1-047) and Tier1 grant (Grant No. RG 113/16), C.-W.Q. contributed to Section 6 only and acknowledges the financial support from A*STAR Pharos Programme (Grant No. 152 70 00014, with Project No. R-263-000-B91-305). Q.O. acknowledges the scholarship support from the MCATM and the FLEET.

Conflict of Interest

The authors declare no conflict of interest.

Keywords

2D materials, hybrid perovskites, nanolasers, optoelectronics, photonics

Received: February 18, 2018
Revised: April 6, 2018
Published online: June 27, 2018

[1] W. Li, Z. Wang, F. Deschler, S. Gao, R. H. Friend, A. K. Cheetham, *Nat. Rev. Mater.* **2017**, *2*, 16099.
[2] T. M. Brenner, D. A. Egger, L. Kronik, G. Hodes, D. Cahen, *Nat. Rev. Mater.* **2016**, *1*, 15007.
[3] J. Berry, T. Buonassisi, D. A. Egger, G. Hodes, L. Kronik, Y. L. Loo, I. Lubomirsky, S. R. Marder, Y. Mastai, J. S. Miller, *Adv. Mater.* **2015**, *27*, 5102.
[4] M. Grätzel, *Nat. Mater.* **2014**, *13*, 838.
[5] D. E. Scaife, P. F. Weller, W. G. Fisher, *J. Solid State Chem.* **1974**, *9*, 308.
[6] K. Yamada, S. Funabiki, H. Horimoto, T. Matsui, T. Okuda, S. Ichiba, *Chem. Lett.* **1991**, *20*, 801.
[7] F. Hao, C. C. Stoumpos, D. H. Cao, R. P. Chang, M. G. Kanatzidis, *Nat. Photonics* **2014**, *8*, 489.
[8] D. B. Mitzi, *Prog. Inorg. Chem.* **2007**, *48*, 1.
[9] I. Chung, J.-H. Song, J. Im, J. Androulakis, C. D. Malliakas, H. Li, A. J. Freeman, J. T. Kenney, M. G. Kanatzidis, *J. Am. Chem. Soc.* **2012**, *134*, 8579.
[10] A. Kojima, K. Teshima, Y. Shirai, T. Miyasaka, *J. Am. Chem. Soc.* **2009**, *131*, 6050.
[11] Y. Zhao, K. Zhu, *Chem. Soc. Rev.* **2016**, *45*, 655.
[12] Y. Zhang, J. Liu, Z. Wang, Y. Xue, Q. Ou, L. Polavarapu, J. Zheng, X. Qi, Q. Bao, *Chem. Commun.* **2016**, *52*, 13637.
[13] S.-T. Ha, R. Su, J. Xing, Q. Zhang, Q. Xiong, *Chem. Sci.* **2017**, *8*, 2522.
[14] J. Song, J. Li, X. Li, L. Xu, Y. Dong, H. Zeng, *Adv. Mater.* **2015**, *27*, 7162.
[15] X. Hu, X. Zhang, L. Liang, J. Bao, S. Li, W. Yang, Y. Xie, *Adv. Funct. Mater.* **2014**, *24*, 7373.
[16] Y. Zhang, J. Du, X. Wu, G. Zhang, Y. Chu, D. Liu, Y. Zhao, Z. Liang, J. Huang, *ACS Appl. Mater. Interfaces* **2015**, *7*, 21634.
[17] Z.-K. Tan, R. S. Moghaddam, M. L. Lai, P. Docampo, R. Higler, F. Deschler, M. Price, A. Sadhanala, L. M. Pazos, D. Credgington, F. Hanusch, T. Bein, H. J. Snaith, R. H. Friend, *Nat. Nanotechnol.* **2014**, *9*, 687.
[18] H. Cho, S.-H. Jeong, M.-H. Park, Y.-H. Kim, C. Wolf, C.-L. Lee, J. H. Heo, A. Sadhanala, N. Myoung, S. Yoo, S. H. Im, R. H. Friend, T.-W. Lee, *Science* **2015**, *350*, 1222.
[19] A. K. Geim, K. S. Novoselov, *Nat. Mater.* **2007**, *6*, 183.
[20] K. Novoselov, D. Jiang, F. Schedin, T. Booth, V. Khotkevich, S. Morozov, A. Geim, *Proc. Natl. Acad. Sci. USA* **2005**, *102*, 10451.
[21] K. Novoselov, A. Mishchenko, A. Carvalho, A. C. Neto, *Science* **2016**, *353*, aac9439.
[22] L. Li, Y. Yu, G. J. Ye, Q. Ge, X. Ou, H. Wu, D. Feng, X. H. Chen, Y. Zhang, *Nat. Nanotechnol.* **2014**, *9*, 372.
[23] E. S. Reich, *Nature* **2014**, *506*, 19.
[24] P. Vogt, P. De Padova, C. Quaresima, J. Avila, E. Frantzeskakis, M. C. Asensio, A. Resta, B. Ealet, G. Le Lay, *Phys. Rev. Lett.* **2012**, *108*, 155501.
[25] L. Tao, E. Cinquanta, D. Chiappe, C. Grazianetti, M. Fanciulli, M. Dubey, A. Molle, D. Akinwande, *Nat. Nanotechnol.* **2015**, *10*, 227.
[26] C. R. Dean, A. F. Young, I. Meric, C. Lee, L. Wang, S. Sorgenfrei, K. Watanabe, T. Taniguchi, P. Kim, K. Shepard, *Nat. Nanotechnol.* **2010**, *5*, 722.
[27] M. Yankowitz, J. Xue, D. Cormode, J. D. Sanchez-Yamagishi, K. Watanabe, T. Taniguchi, P. Jarillo-Herrero, P. Jacquod, B. J. LeRoy, *Nat. Phys.* **2012**, *8*, 382.
[28] H. Wang, H. Yuan, S. S. Hong, Y. Li, Y. Cui, *Chem. Soc. Rev.* **2015**, *44*, 2664.
[29] K. F. Mak, C. Lee, J. Hone, J. Shan, T. F. Heinz, *Phys. Rev. Lett.* **2010**, *105*, 136805.
[30] F. Bonaccorso, Z. Sun, T. Hasan, A. Ferrari, *Nat. Photonics* **2010**, *4*, 611.
[31] Q. Bao, K. P. Loh, *ACS Nano* **2012**, *6*, 3677.
[32] G. Eda, S. A. Maier, *ACS Nano* **2013**, *7*, 5660.
[33] Q. H. Wang, K. Kalantar-Zadeh, A. Kis, J. N. Coleman, M. S. Strano, *Nat. Nanotechnol.* **2012**, *7*, 699.
[34] F. Xia, H. Wang, D. Xiao, M. Dubey, A. Ramasubramaniam, *Nat. Photonics* **2014**, *8*, 899.
[35] J.-C. Blancon, H. Tsai, W. Nie, C. Stoumpos, L. Pedesseau, C. Katan, M. Kepenekian, C. Soe, K. Appavoo, M. Sfeir, *Science* **2017**, *355*, 1288.
[36] H. Tsai, W. Nie, J.-C. Blancon, C. C. Stoumpos, R. Asadpour, B. Harutyunyan, A. J. Neukirch, R. Verduzco, J. J. Crochet, S. Tretiak, *Nature* **2016**, *536*, 312.
[37] D. Mitzi, S. Wang, C. Feild, C. Chess, A. Guloy, *Science* **1995**, *267*, 1473.
[38] D. B. Mitzi, C. Feild, W. Harrison, A. Guloy, *Nature* **1994**, *369*, 467.
[39] F. Hao, C. C. Stoumpos, R. P. Chang, M. G. Kanatzidis, *J. Am. Chem. Soc.* **2014**, *136*, 8094.
[40] M. A. Green, A. Ho-Baillie, H. J. Snaith, *Nat. Photonics* **2014**, *8*, 506.
[41] L. Dou, A. B. Wong, Y. Yu, M. Lai, N. Kornienko, S. W. Eaton, A. Fu, C. G. Bischak, J. Ma, T. Ding, N. S. Ginsberg, L.-W. Wang, A. P. Alivisatos, P. Yang, *Science* **2015**, *349*, 1518.
[42] H. Tan, A. Jain, O. Voznyy, X. Lan, F. P. G. de Arquer, J. Z. Fan, R. Quintero-Bermudez, M. Yuan, B. Zhang, Y. Zhao, *Science* **2017**, *355*, 722.
[43] J. A. Sichert, Y. Tong, N. Mutz, M. Vollmer, S. Fischer, K. Z. Milowska, R. García Cortadella, B. Nickel, C. Cardenas-Daw, J. K. Stolarczyk, A. S. Urban, J. Feldmann, *Nano Lett.* **2015**, *15*, 6521.
[44] S.-T. Ha, C. Shen, J. Zhang, Q. Xiong, *Nat. Photonics* **2016**, *10*, 115.
[45] J. Liu, Y. Xue, Z. Wang, Z.-Q. Xu, C. Zheng, B. Weber, J. Song, Y. Wang, Y. Lu, Y. Zhang, Q. Bao, *ACS Nano* **2016**, *10*, 3536.
[46] S. Nah, B. Spokoyny, C. Stoumpos, C. Soe, M. Kanatzidis, E. Harel, *Nat. Photonics* **2017**, *11*, 285.
[47] L. Mao, Y. Wu, C. C. Stoumpos, M. R. Wasielewski, M. G. Kanatzidis, *J. Am. Chem. Soc.* **2017**, *139*, 5210.
[48] B. R. Sutherland, E. H. Sargent, *Nat. Photonics* **2016**, *10*, 295.

[49] H.-R. Wenk, A. Bulakh, *Minerals: Their Constitution and Origin*, Cambridge University Press, New York, NY **2004**.
[50] D. B. Mitzi, *J. Chem. Soc., Dalton Trans.* **2001**, *1*, 1.
[51] D. Weber, *Z. Naturforsch., B* **1978**, *33*, 1443.
[52] A. Poglitsch, D. Weber, *J. Chem. Phys.* **1987**, *87*, 6373.
[53] Y. Zhao, K. Zhu, *Chem. Soc. Rev.* **2016**, *45*, 655.
[54] Q. Chen, N. De Marco, Y. Yang, T.-B. Song, C.-C. Chen, H. Zhao, Z. Hong, H. Zhou, Y. Yang, *Nano Today* **2015**, *10*, 355.
[55] S. T. Ha, X. Liu, Q. Zhang, D. Giovanni, T. C. Sum, Q. Xiong, *Adv. Opt. Mater.* **2014**, *2*, 838.
[56] L. Su, Z. X. Zhao, H. Y. Li, J. Yuan, Z. L. Wang, G. Z. Cao, G. Zhu, *ACS Nano* **2015**, *9*, 11310.
[57] J. Song, L. Xu, J. Li, J. Xue, Y. Dong, X. Li, H. Zeng, *Adv. Mater.* **2016**, *28*, 4861.
[58] Z. Fan, H. Xiao, Y. Wang, Z. Zhao, Z. Lin, H.-C. Cheng, S.-J. Lee, G. Wang, Z. Feng, W. A. Goddard III, Y. Huang, X. Duan, *Joule* **2017**, *1*, 548.
[59] W. Xu, J. A. McLeod, Y. Yang, Y. Wang, Z. Wu, S. Bai, Z. Yuan, T. Song, Y. Wang, J. Si, R. Wang, X. Gao, X. Zhang, L. Liu, B. Sun, *ACS Appl. Mater. Interfaces* **2016**, *8*, 23181.
[60] V. G. -Pedro, E.-J. Juarez-Perez, W. S. Arsyad, E. M. Barea, F. F. Santiago, Ivan M. -Sero, J. Bisquert, *Nano Lett.* **2014**, *14*, 888.
[61] G. R. Li, F. W. R. Rivarola, N. J. L.-K. Davis, S. Bai, T.-C. Jellicoe, F. de la Peña, S. C. Hou, C. Ducati, F. Gao, R. H. Friend, N. C. Greenham, Z.-K. Tan, *Adv. Mater.* **2016**, *28*, 3528.
[62] J. Wang, N. Wang, Y. Jin, J. Si, Z. K. Tan, H. Du, L. Cheng, X. Dai, S. Bai, H. He, *Adv. Mater.* **2015**, *27*, 2311.
[63] W. L. Hong, Y. C. Huang, C. Y. Chang, Z. C. Zhang, H. R. Tsai, N. Y. Chang, Y. C. Chao, *Adv. Mater.* **2016**, *28*, 8029.
[64] S. G. R. Bade, J. Li, X. Shan, Y. Ling, Y. Tian, T. Dilbeck, T. Besara, T. Geske, H. Gao, B. Ma, *ACS Nano* **2016**, *10*, 1795.
[65] X. Zhang, H. Lin, H. Huang, C. Reckmeier, Y. Zhang, W. C. Choy, A. L. Rogach, *Nano Lett.* **2016**, *16*, 1415.
[66] S. A. Veldhuis, P. P. Boix, N. Yantara, M. Li, T. C. Sum, N. Mathews, S. G. Mhaisalkar, *Adv. Mater.* **2016**, *28*, 6804.
[67] D. Liang, Y. Peng, Y. Fu, M. J. Shearer, J. Zhang, J. Zhai, Y. Zhang, R. J. Hamers, T. L. Andrew, S. Jin, *ACS Nano* **2016**, *10*, 6897.
[68] N. Yantara, S. Bhaumik, F. Yan, D. Sabba, H. A. Dewi, N. Mathews, P. P. Boix, H. V. Demir, S. Mhaisalkar, *J. Phys. Chem. Lett.* **2015**, *6*, 4360.
[69] Q. Zhang, S. T. Ha, X. Liu, T. C. Sum, Q. Xiong, *Nano Lett.* **2014**, *14*, 5995.
[70] P. Li, Y. Chen, T. Yang, Z. Wang, H. Lin, Y. Xu, L. Li, H. Mu, B. N. Shivananju, Y. Zhang, Q. Zhang, A. Pan, S. Li, D. Tang, B. Jia, H. Zhang, Q. Bao, *ACS Appl. Mater. Interfaces* **2017**, *9*, 12759.
[71] M. Yuan, L. N. Quan, R. Comin, G. Walters, R. Sabatini, O. Voznyy, S. Hoogland, Y. Zhao, E. M. Beauregard, P. Kanjanaboos, Z. Lu, D. H. Kim, E. H. Sargent, *Nat. Nanotechnol.* **2016**, *11*, 872.
[72] I. Borriello, G. Cantele, D. Ninno, *Phys. Rev. B* **2008**, *77*, 235214.
[73] Y. Wang, X. Li, X. Zhao, L. Xiao, H. Zeng, H. Sun, *Nano Lett.* **2016**, *16*, 448.
[74] Y. Wang, T. Gould, J. F. Dobson, H. Zhang, H. Yang, X. Yao, H. Zhao, *Phys. Chem. Chem. Phys.* **2014**, *16*, 1424.
[75] E. Mosconi, A. Amat, M. K. Nazeeruddin, M. Grätzel, F. De Angelis, *J. Phys. Chem. C* **2013**, *117*, 13902.
[76] J. H. Noh, S. H. Im, J. H. Heo, T. N. Mandal, S. I. Seok, *Nano Lett.* **2013**, *13*, 1764.
[77] C. C. Stoumpos, C. D. Malliakas, M. G. Kanatzidis, *Inorg. Chem.* **2013**, *52*, 9019.
[78] F. Hao, C. C. Stoumpos, D. H. Cao, R. P. H. Chang, M. G. Kanatzidis, *Nat. Photonics* **2014**, *8*, 489.
[79] N. K. Noel, S. D. Stranks, A. Abate, C. Wehrenfennig, S. Guarnera, A.-A. Haghighirad, A. Sadhanala, G. E. Eperon, S. K. Pathak, M. B. Johnston, A. Petrozza, L. M. Herz, H. J. Snaith, *Energy Environ. Sci.* **2014**, *7*, 3061.
[80] K. S. Novoselov, A. K. Geim, S. V. Morozov, D. Jiang, M. I. Katsnelson, I. V. Grigorieva, S. V. Dubonos, A. A. Firsov, *Nature* **2005**, *438*, 197.
[81] L. Li, Y. Yu, G. J. Ye, Q. Ge, X. Ou, H. Wu, D. Feng, X. H. Chen, Y. Zhang, *Nat. Nanotechnol.* **2014**, *9*, 372.
[82] S. B. Desai, S. R. Madhvapathy, A. B. Sachid, J. P. Llinas, Q. Wang, G. H. Ahn, G. Pitner, M. J. Kim, J. Bokor, C. Hu, H.-S. P. Wong, A. Javey, *Science* **2016**, *354*, 99.
[83] A. Miyata, A. Mitioglu, P. Plochocka, O. Portugall, J. T.-W. Wang, S. D. Stranks, H. J. Snaith, R. J. Nicholas, *Nat. Phys.* **2015**, *11*, 582.
[84] K. Zheng, Q. Zhu, M. Abdellah, M. E. Messing, W. Zhang, A. Generalov, Y. Niu, L. Ribaud, S. E. Canton, T. Pullerits, *J. Phys. Chem. Lett.* **2015**, *6*, 2969.
[85] Q. Dong, Y. Fang, Y. Shao, P. Mulligan, J. Qiu, L. Cao, J. Huang, *Science* **2015**, *347*, 967.
[86] L. M. Pazos-Outón, M. Szumilo, R. Lamboll, J. M. Richter, M. Crespo-Quesada, M. Abdi-Jalebi, H. J. Beeson, M. Vrućinić, M. Alsari, H. J. Snaith, B. Ehrler, R. H. Friend, F. Deschler, *Science* **2016**, *351*, 1430.
[87] Y. Fang, H. Wei, Q. Dong, J. Huang, *Nat. Commun.* **2017**, *8*, 14417.
[88] J. Peng, Y. Chen, K. Zheng, T. Pullerits, Z. Liang, *Chem. Soc. Rev.* **2017**, *46*, 5714.
[89] M. Amani, D.-H. Lien, D. Kiriya, J. Xiao, A. Azcatl, J. Noh, S. R. Madhvapathy, R. Addou, S. KC, M. Dubey, K. Cho, R. M. Wallace, S.-C. Lee, J.-H. He, J. W. Ager, X. Zhang, E. Yablonovitch, A. Javey, *Science* **2015**, *350*, 1065.
[90] H. Wang, C. Zhang, F. Rana, *Nano Lett.* **2015**, *15*, 339.
[91] H. Chen, J. Yang, E. Rusak, J. Straubel, R. Guo, Y. W. Myint, J. Pei, M. Decker, I. Staude, C. Rockstuhl, Y. Lu, Y. S. Kivshar, D. Neshev, *Sci. Rep.* **2016**, *6*, 22296.
[92] D. Hanlon, C. Backes, E. Doherty, C. S. Cucinotta, N. C. Berner, C. Boland, K. Lee, A. Harvey, P. Lynch, Z. Gholamvand, S. Zhang, K. Wang, G. Moynihan, A. Pokle, Q. M. Ramasse, N. McEvoy, W. J. Blau, J. Wang, G. Abellan, F. Hauke, A. Hirsch, S. Sanvito, D. D. O'Regan, G. S. Duesberg, V. Nicolosi, J. N. Coleman, *Nat. Commun.* **2015**, *6*, 8563.
[93] Y. Zhang, Y. Wang, Z.-Q. Xu, J. Liu, J. Song, Y. Xue, Z. Wang, J. Zheng, L. Jiang, C. Zheng, *ACS Nano* **2016**, *10*, 7031.
[94] Z. Xiao, Y. Yuan, Y. Shao, Q. Wang, Q. Dong, C. Bi, P. Sharma, A. Gruverman, J. Huang, *Nat. Mater.* **2015**, *14*, 193.
[95] Y. Yuan, J. Huang, *Acc. Chem. Res.* **2016**, *49*, 286.
[96] P. Hosseini, C. D. Wright, H. Bhaskaran, *Nature* **2014**, *511*, 206.
[97] L. Dou, *J. Mater. Chem. C* **2017**, *5*, 11165.
[98] S. Chen, G. Shi, *Adv. Mater.* **2017**, *29*, 1605448.
[99] H.-C. Cheng, G. Wang, D. Li, Q. He, A. Yin, Y. Liu, H. Wu, M. Ding, Y. Huang, X. Duan, *Nano Lett.* **2016**, *16*, 367.
[100] L. Niu, X. Liu, C. Cong, C. Wu, D. Wu, T. R. Chang, H. Wang, Q. Zeng, J. Zhou, X. Wang, W. Fu, P. Yu, Q. Fu, S. Najmaei, Z. Zhang, B. I. Yakobson, B. K. Tay, W. Zhou, H. T. Jeng, H. Lin, T. C. Sum, C. Jin, H. He, T. Yu, Z. Liu, *Adv. Mater.* **2015**, *27*, 7800.
[101] Y. Lee, J. Kwon, E. Hwang, C. H. Ra, W. J. Yoo, J. H. Ahn, J. H. Park, J. H. Cho, *Adv. Mater.* **2015**, *27*, 41.
[102] G. Volonakis, F. Giustino, *J. Phys. Chem. Lett.* **2015**, *6*, 2496.
[103] D. M. Jang, K. Park, D. H. Kim, J. Park, F. Shojaei, H. S. Kang, J.-P. Ahn, J. W. Lee, J. K. Song, *Nano Lett.* **2015**, *15*, 5191.
[104] L. Dou, M. Lai, C. S. Kley, Y. Yang, C. G. Bischak, D. Zhang, S. W. Eaton, N. S. Ginsberg, P. Yang, *Proc. Natl. Acad. Sci. USA* **2017**, *114*, 7216.
[105] D. Jariwala, T. J. Marks, M. C. Hersam, *Nat. Mater.* **2017**, *16*, 170.
[106] Y. Liu, N. O. Weiss, X. Duan, H.-C. Cheng, Y. Huang, X. Duan, *Nat. Rev. Mater.* **2016**, *1*, 16042.
[107] C. J. Docherty, P. Parkinson, H. J. Joyce, M.-H. Chiu, C.-H. Chen, M.-Y. Lee, L.-J. Li, L. M. Herz, M. B. Johnston, *ACS Nano* **2014**, *8*, 11147.

[108] H. Wei, Y. Fang, P. Mulligan, W. Chuirazzi, H.-H. Fang, C. Wang, B. Ecker, Y. Gao, M. Loi, L. Cao, J. Huang, *Nat. Photonics* **2016**, *10*, 333.
[109] W. Pan, H. Wu, J. Luo, Z. Deng, C. Ge, C. Chen, X. Jiang, W.-J. Yin, G. Niu, L. Zhu, L. Yin, Y. Zhou, Q. Xie, X. Ke, M. Sui, J. Tang, *Nat. Photonics* **2017**, *11*, 726.
[110] Q. Ou, Y. Zhang, Z. Wang, J. A. Yuwono, R. Wang, Z. Dai, W. Li, C. Zheng, Z.-Q. Xu, X. Qi, S. Duhm, N. V. Medhekar, H. Zhang, Q. Bao, *Adv. Mater.* **2018**, *30*, 1705792.
[111] Z. Tan, Y. Wu, H. Hong, J. Yin, J. Zhang, L. Lin, M. Wang, X. Sun, L. Sun, Y. Huang, K. Liu, Z. Liu, H. Peng, *J. Am. Chem. Soc.* **2016**, *138*, 16612.
[112] Y. X. Yang, G. L. Yuan, Z. B. Yan, Y. J. Wang, X. B. Lu, J.-M. Liu, *Adv. Mater.* **2017**, *29*, 1700425.
[113] G. Xu, R. Lu, J. Liu, H. Y. Chiu, R. Hui, J. Z. Wu, *Adv. Opt. Mater.* **2014**, *2*, 729.
[114] S. Zhang, M. Xie, F. Li, Z. Yan, Y. Li, E. Kan, W. Liu, Z. Chen, H. Zeng, *Angew. Chem., Int. Ed.* **2016**, *55*, 1666.
[115] R. Dong, Y. Fang, J. Chae, J. Dai, Z. Xiao, Q. Dong, Y. Yuan, A. Centrone, X. C. Zeng, J. Huang, *Adv. Mater.* **2015**, *27*, 1912.
[116] L. Dou, Y. M. Yang, J. You, Z. Hong, W. H. Chang, G. Li, Y. Yang, *Nat. Commun.* **2014**, *5*, 5404.
[117] Y. Fang, J. Huang, *Adv. Mater.* **2015**, *27*, 2804.
[118] P. Li, D. S. B N, Y. Zhang, S. Li, Q. Bao, *J. Phys. D: Appl. Phys.* **2017**, *50*, 094002.
[119] J. T.-W. Wang, J. M. Ball, E. M. Barea, A. Abate, J. A. Alexander-Webber, J. Huang, M. Saliba, I. Mora-Sero, J. Bisquert, H. J. Snaith, R. J. Nicholas, *Nano Lett.* **2014**, *14*, 724.
[120] Z. Zhu, J. Ma, Z. Wang, C. Mu, Z. Fan, L. Du, Y. Bai, L. Fan, H. Yan, D. L. Phillips, S. Yang, *J. Am. Chem. Soc.* **2014**, *136*, 3760.
[121] O. Ergen, S. M. Gilbert, T. Pham, S.-J. Turner, M. T. -Zhi Tan, M. A. Worsley, A. Zettl, *Nat. Mater.* **2017**, *16*, 522.
[122] L. Meng, J. You, T.-F. Guo, Y. Yang, *Acc. Chem. Res.* **2016**, *49*, 155.
[123] Q. Chen, N. De Marco, Y. M. Yang, T.-B. Song, C.-C. Chen, H. Zhao, Z. Hong, H. Zhou, Y. Yang, *Nano Today* **2015**, *10*, 355.
[124] G. Niu, X. Guo, L. Wang, *J. Mater. Chem. A* **2015**, *3*, 8970.
[125] W. S. Yang, B.-W. Park, E. H. Jung, N. J. Jeon, Y. C. Kim, D. U. Lee, S. S. Shin, J. Seo, E. K. Kim, J. H. Noh, *Science* **2017**, *356*, 1376.
[126] I. C. Smith, E. T. Hoke, D. Solis-Ibarra, M. D. McGehee, H. I. Karunadasa, *Angew. Chem., Int. Ed.* **2014**, *53*, 11232.
[127] H. Tsai, W. Nie, J. C. Blancon, C. C. Stoumpos, R. Asadpour, B. Harutyunyan, A. J. Neukirch, R. Verduzco, J. J. Crochet, S. Tretiak, L. Pedesseau, J. Even, M. A. Alam, G. Gupta, J. Lou, P. M. Ajayan, M. J. Bedzyk, M. G. Kanatzidis, A. D. Mohite, *Nature* **2016**, *536*, 312.
[128] Z. Wang, Q. Lin, F. P. Chmiel, N. Sakai, L. M. Herz, H. J. Snaith, *Nat. Energy* **2017**, *6*, 17135.
[129] J.-C. Blancon, H. Tsai, W. Nie, C. C. Stoumpos, L. Pedesseau, C. Katan, M. Kepenekian, C. M. M. Soe, K. Appavoo, M. Y. Sfeir, S. Tretiak, P. M. Ajayan, M. G. Kanatzidis, J. Even, J. J. Crochet, A. D. Mohite, *Science* **2017**, *355*, 1288.
[130] P. Löper, B. Niesen, S.-J. Moon, S. M. De Nicolas, J. Holovsky, Z. Remes, M. Ledinsky, F.-J. Haug, J.-H. Yum, S. De Wolf, *IEEE J. Photovolt.* **2014**, *4*, 1545.
[131] E. T. Hoke, D. J. Slotcavage, E. R. Dohner, A. R. Bowring, H. I. Karunadasa, M. D. McGehee, *Chem. Sci.* **2015**, *6*, 613.
[132] G. E. Eperon, T. Leijtens, K. A. Bush, R. Prasanna, T. Green, J. T.-W. Wang, D. P. McMeekin, G. Volonakis, R. L. Milot, R. May, *Science* **2016**, *354*, 861.
[133] A. Miyata, A. Mitioglu, P. Plochocka, O. Portugall, J. T.-W. Wang, S. D. Stranks, H. J. Snaith, R. J. Nicholas, *Nat. Phys.* **2015**, *11*, 582.
[134] M. Era, S. Morimoto, T. Tsutsui, S. Saito, *Appl. Phys. Lett.* **1994**, *65*, 676.
[135] Y. Ling, Z. Yuan, Y. Tian, X. Wang, J. C. Wang, Y. Xin, K. Hanson, B. Ma, H. Gao, *Adv. Mater.* **2016**, *28*, 305.
[136] N. Wang, L. Cheng, R. Ge, S. Zhang, Y. Miao, W. Zou, C. Yi, Y. Sun, Y. Cao, R. Yang, Y. Wei, Q. Guo, Y. Ke, M. Yu, Y. Jin, Y. Liu, Q. Ding, D. Di, L. Yang, G. Xing, H. Tian, C. Jin, F. Gao, R. H. Friend, J. Wang, W. Huang, *Nat. Photonics* **2016**, *10*, 699.
[137] F. Withers, O. Del Pozo-Zamudio, A. Mishchenko, A. Rooney, A. Gholinia, K. Watanabe, T. Taniguchi, S. Haigh, A. Geim, A. Tartakovskii, *Nat. Mater.* **2015**, *14*, 301.
[138] R. L. Milot, R. J. Sutton, G. E. Eperon, A. A. Haghighirad, J. M. Hardigree, L. Miranda, H. J. Snaith, M. B. Johnston, L. M. Herz, *Nano Lett.* **2016**, *16*, 7001.
[139] G. Xing, N. Mathews, S. S. Lim, N. Yantara, X. Liu, D. Sabba, M. Grätzel, S. Mhaisalkar, T. C. Sum, *Nat. Mater.* **2014**, *13*, 476.
[140] F. Deschler, M. Price, S. Pathak, L. E. Klintberg, D. D. Jarausch, R. Higler, S. Huttner, T. Leijtens, S. D. Stranks, H. J. Snaith, M. Atature, R. T. Phillips, R. H. Friend, *J. Phys. Chem. Lett.* **2014**, *5*, 1421.
[141] Q. Zhang, R. Su, X. Liu, J. Xing, T. C. Sum, Q. Xiong, *Adv. Funct. Mater.* **2016**, *26*, 6238.
[142] H. Zhu, Y. Fu, F. Meng, X. Wu, Z. Gong, Q. Ding, M. V. Gustafsson, M. T. Trinh, S. Jin, X. Zhu, *Nat. Mater.* **2015**, *14*, 636.
[143] Q. Zhang, R. Su, W. Du, X. Liu, L. Zhao, S. T. Ha, Q. Xiong, *Small Methods* **2017**, *1*, 1700163.
[144] M. S. Alias, I. Dursun, D. Shi, M. I. Saidaminov, E. M. Diallo, D. Priante, T. K. Ng, O. M. Bakr, B. S. Ooi, *J. Vac. Sci. Technol., B* **2015**, *33*, 051207.
[145] M. S. Alias, Y. Yang, T. K. Ng, I. Dursun, D. Shi, M. I. Saidaminov, D. Priante, O. M. Bakr, B. S. Ooi, *J. Phys. Chem. Lett.* **2015**, *7*, 137.
[146] Z. Wang, J. Liu, Z.-Q. Xu, Y. Xue, L. Jiang, J. Song, F. Huang, Y. Wang, Y. L. Zhong, Y. Zhang, Y.-B. Cheng, Q. Bao, *Nanoscale* **2016**, *8*, 6258.
[147] W. Mao, J. Zheng, Y. Zhang, A. S. R. Chesman, Q. Ou, J. Hicks, F. Li, Z. Wang, B. Graystone, T. D. M. Bell, M. U. Rothmann, N. W. Duffy, L. Spiccia, Y.-B. Cheng, Q. Bao, U. Bach, *Angew. Chem., Int. Ed.* **2017**, *56*, 12486.
[148] E. Mosconi, A. Amat, M. K. Nazeeruddin, M. Grätzel, F. De Angelis, *J. Phys. Chem. C* **2013**, *117*, 13902.
[149] R. Zhang, J. Fan, X. Zhang, H. Yu, H. Zhang, Y. Mai, T. Xu, J. Wang, H. J. Snaith, *ACS Photonics* **2016**, *3*, 371.
[150] B. S. Kalanoor, L. Gouda, R. Gottesman, S. Tirosh, E. Haltzi, A. Zaban, Y. R. Tischler, *ACS Photonics* **2016**, *3*, 361.
[151] J. C. Johnson, Z. Li, P. F. Ndione, K. Zhu, *J. Mater. Chem. C* **2016**, *4*, 4847.
[152] G. Walters, B. R. Sutherland, S. Hoogland, D. Shi, R. Comin, D. P. Sellan, O. M. Bakr, E. H. Sargent, *ACS Nano* **2015**, *9*, 9340.
[153] W. G. Lu, C. Chen, D. Han, L. Yao, J. Han, H. Zhong, Y. Wang, *Adv. Opt. Mater.* **2016**, *4*, 1732.
[154] Y. Xu, Q. Chen, C. Zhang, R. Wang, H. Wu, X. Zhang, G. Xing, W. W. Yu, X. Wang, Y. Zhang, *J. Am. Chem. Soc.* **2016**, *138*, 3761.
[155] Y. W, X. Li, X. Zhao, L. Xiao, H. Zeng, H. Sun, *Nano Lett.* **2015**, *16*, 448.
[156] J. Du, Q. Wang, G. Jiang, C. Xu, C. Zhao, Y. Xiang, Y. Chen, S. Wen, H. Zhang, *Sci. Rep.* **2014**, *4*, 6346.
[157] Q. Bao, H. Zhang, Y. Wang, Z. Ni, Y. Yan, Z. X. Shen, K. P. Loh, D. Y. Tang, *Adv. Funct. Mater.* **2009**, *19*, 3077.
[158] A. Savoia, D. Paparo, P. Perna, Z. Ristic, M. Salluzzo, F. M. Granozio, U. S. di Uccio, C. Richter, S. Thiel, J. Mannhart, *Phys. Rev. B* **2009**, *80*, 075110.
[159] X. Zheng, Y. Liu, G. Liu, J. Liu, X. Ye, Q. Han, C. Ge, X. Tao, *Chem. Mater.* **2016**, *28*, 4421.
[160] C. Zhang, K. Wang, N. Yi, Y. Gao, M. Zhu, W. Sun, S. Liu, K. Xu, S. Xiao, Q. Song, *Adv. Opt. Mater.* **2016**, *4*, 2057.
[161] A. M. A. Leguy, J. M. Frost, A. P. McMahon, V. G. Sakai, W. Kockelmann, C. Law, X. Li, F. Foglia, A. Walsh, B. C. O'Regan, J. Nelson, J. T. Cabral, P. R. F. Barnes, *Nat. Commun.* **2015**, *6*, 7124.